AES2006

A Novel Application for Ultrasound as an Emulsification Mechanism within the Oil Industry

A Controlled Experiment

December 2009

Pieter Huibert Kool

TU Delft

Department of Geotechnology

Delft University of Technology

Title	:	**A Novel Application for Ultrasound as an Emulsification Mechanism within the Oil Industry**
Author(s)	:	Pieter Huibert Kool
Date	:	December 2009
Professor(s)	:	Prof. Dr. P.L.J. Zitha, Dr. Ir. D.M.J. Smeulders
Supervisor(s)	:	Prof. W.R. Rossen, Dr. Ir. E.S.J. Rudolph
TA Report number	:	AES/2006
Postal Address	:	Section for Petroleum Engineering Department of Applied Earth Sciences Delft University of Technology P.O. Box 5028 The Netherlands
Telephone	:	(31) 15 2781328 (secretary)
Telefax	:	(31) 15 2781189

Acknowledgment

I would like to thank the following people for the help and support in bringing my thesis to a successful conclusion: Susanne Rudolph for always making time to help me even when she already had ten other things planned. Bill Rossen for taking part of my committee. Karel Heller and Adri Maljaars, for help with the ultrasonic bath (and taking it apart). Ellen Meijvogel and Jolanda van Haagen for aiding me with some of the experiments and occasionally overlooking the huge mess I made in the laboratory. Niels and Menno for commenting me on my writing and of course Joris, Douglas, Claartje, Tuur and the other Msc for taking me out for coffee once in a while. Ben Norder with his help on the TGA and Gerard de Vos with his help with the SEM.
And last but not least my supervisors Pacelli Zitha and David Smeulders without whom this never would have come to a successful ending.

Thank you all!

Abstract

Ultrasound has a number of applications within Enhanced Oil Recovery (EOR). Most of these are focused on down hole cleaning. An alternative use of ultrasound is creating emulsions with the purpose of mobility control.

The goal of this study is to observe the effect of ultrasound on the emulsification of oil and water. For the experiments that were covered in this study an ultrasonic bath was used. Characterizing the energy distribution within the ultrasonic tank was the first crucial step. It was observed that salt dissolution was enhanced as a result of sonication. The dissolution was used as a measure for the local energy intensity. A significant amount of salt had gone into dissolution as a result of sonication. This is a novel method to characterize the energy distribution of an ultrasonic bath

Two high energy regimes that were localized with the dissolution method were used for the emulsification of the oil and water. A rang of surfactant concentrations were tested.

The goal was to study the effect of a varying surfactant (alpha-olefin-sulphonate) concentration on the result of the emulsification process of hexadecane and water. After filling a test tube with a surfactant solution and oil and positioning it in the previously localized high energy spot in the ultrasonic bath the sample was sonicated. After 30 minutes of sonication, either an emulsion or a gel-like substance was observed between the surfactant solution and the oil. It had been observed that the type and quantity of this “middle substance” depends on the surfactant concentration. The gels that were recovered from the test tubes were freeze-dried and analyzed with a scanning electron microscope. The gel has a dual porosity. The large-scale pores have a spherical shape and are 50-500 µm in diameter. The smaller pores are shaped as wormholes. They are 1-3 µm in diameter.

The gel could prove useful for near-wellbore applications. The emulsions form easily under the acoustic stimulation, hence application to mobility control or other EOR related applications is thought feasible.

Table of contents

1. Introduction

Due to the limitations of the current Enhanced Oil Recovery (EOR) methods a substantial amount of the oil is not recoverable. It is not surprising that research has focused on improving existing recovery mechanisms and finding new ones.

It was noted that the oil production occasionally peaked after an earthquake[1]. Laboratory experiments and the production data after such incidents have shown that low-frequency (<500 Hz) acoustic waves can enhance the mobility of oil and thus the total oil recovery in a mature oil field[2]. Field tests with conventional seismic sources have never been able to confirm these results[3].

In addition to low frequencies also high frequency acoustic waves (ultrasound) have been studied as a possible EOR mechanism. Experiments have been performed to prove whether ultrasound can assist in the removal of scale deposits, mud penetration[4] or wax deposits[5].

When oil and water are mixed to form an emulsion, the mobility of both liquids is greatly affected. Depending on e.g., droplet size and pore throat size, the mobility can either increase or decrease[6]. Mobility control is an important strategy in EOR; increasing the mobility can, for instance reduce the residual oil in a mature oil field, thus increasing the recovery factor. On the other hand decreasing the mobility can, for instance, be of use to block thief zones (highly permeable layers in a reservoir). By blocking the thief zones the injected water is diverted and the sweep efficiency of the (mature) reservoir improved[7].

In 2008 during an experiment at the Geotechnology Laboratory of Delft University of Technology, in which it was attempted to emulsify oil and water in an ultrasonic bath using a surfactant, a remarkable observation was made. At the interface between the oil and water phase a gel was formed. The main objective of this thesis is to replicate this, creating a similar gel using ultrasound. Very little is known about the setup of the 2008 experiment. Therefore predicting under which conditions the gel forms is not possible.

For the experiments an ultrasonic bath is used (Chapter 1). To ensure a controlled experiment the energy distribution of the ultrasonic bath is characterized first. It is expected that the acoustic energy can enhance the dissolution of sodium chloride. A higher acoustic energy will therefore lead to a higher dissolution rate. This forms a novel method in charactering an ultrasonic bath.

2. The dissolution of NaCl through ultrasonic stimulation

2.1. Abstract

A goal of this study was to observe if ultrasound enhances the dissolution of sodium chloride (NaCl) in water. Additionally the enhanced dissolution rate could be used to characterize the acoustic energy distribution of an ultrasonic bath.

Test tubes (36) filled with 5.0 ± 0.1g NaCl salt and demineralized water they were placed in and ultrasonic tank an sonicated for 5 mins. An untreated (no sonication) test tube with an identical quantity of salt and water was observed for comparison. The difference in salt column (salt level) height, before and after sonication, was used as a measure for the dissolution (rate).

It was observed that the sonicated test tubes had larger drops in salt level (5.5 mm on average) after 5 mins than an untreated test tube over 20 hrs. It could therefore be concluded that ultrasound had a significant impact on the dissolution rate. Furthermore the drop in salt level of the sonicated test tubes varied significantly with the location in the tank. This suggests that the ultrasonic bath had a heterogeneous energy distribution and that the applied method applied was sensitive enough to detect differences. Some of the treated test tubes had a tilted level of the solid phase after sonication.

It is possible to use the dissolution of NaCl in water to characterize the energy distribution of the ultrasonic bath.

Keywords

[ultrasonic bath, dissolution, Sodium Chloride]

Nomenclature

Δh	*Drop in solid phase level before adding water and after sonication*	*[mm]*
h^d	*Salt level in test tube, with out water*	*[mm]*
h^b	*Salt level height before sonication*	*[mm]*
h^a	*Salt level height after sonication*	*[mm]*
$h_{max}{}^a$	*The maximum measured salt level after sonication*	*[mm]*
$h_{min}{}^a$	*The minimum measured salt level after sonication*	*[mm]*
$h_{avg}{}^a$	*The average height of* h_{max} *and* h_{min}	*[min]*
f	*Relative weight loss due to erosion*	*[-]*
m^b	*Weight of aluminium strip before sonication*	*[g]*
m^a	*Weight of aluminium strip after sonication*	*[g]*
ε	*Experimental error*	*[-]*

2.2. *Introduction*

Ultrasound is used worldwide for different applications including altering the bulk properties of liquids and solid particles (material science),[8] cleaning of substrate surfaces, and laboratory experiments (such is the case for this study)[9]. The objectives of the experiments are to find out if the dissolution of salt is influenced by if this can be used to characterize the ultrasonic bath.

Within an ultrasonic tank, there is a heterogeneous distribution of energy. It is believed that the most important contributing factor to this heterogeneous distribution is interfering sound patterns generated by the transducers[9].

If it is indeed possible that dissolution can be enhanced by ultrasound, it is to be expected that also the dissolution rate will be dependent on the position within the ultrasonic tank.

2.3. *Problem statement and definitions*

Multiple commercial appliances are available that can generate ultrasound. The ultrasonic bath is an example of such an appliance. An ultrasonic bath consists of a container with piezoelectric transducers attached to the outside bottom (Figure 1). The container, is filled with tap- or demi-water. The transducers emit ultrasonic waves into the water. The acoustic pressure waves undergo, alternating pressure cycles.

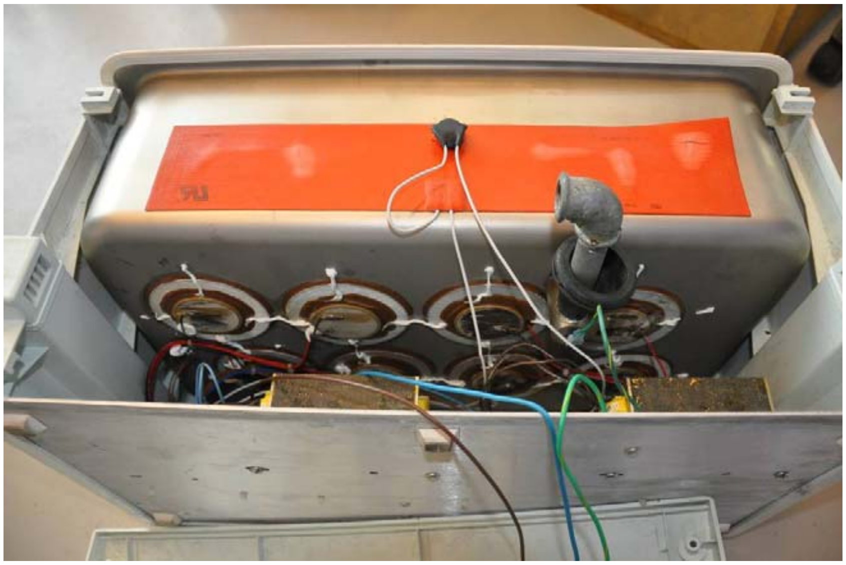

Figure 1: The tank with plastic covers removed. The piezoelectric transducers are clearly visible on bottom of the tank. The orange rectangle is an electric heat source and was not used during experiments.

Cavitation is the phenomenon that occurs when a liquid is "stretched" in the pressure trough of an acoustic wave. When, the pressure (P) falls below the vapour pressure of the liquid (P_v) and the resulting tension (ΔP) is greater than the "*tensile*" strength of the liquid, cavities will be formed[11]. During transient cavitation (a form of cavitation where the formation of a bubble is quickly followed by its violent collapse) extremely high local temperatures and pressures are reached (p~1000 atm, T~5000 K with heating and cooling rates of 10^{10} K/s)[10, 19, 10].

Within a solid-liquid system, ultrasonic cavitation can produce some high-energy phenomena. Important physical effects include[8]: 1) Improved mass transport by turbulent mixing and acoustic streaming, 2) Fragmentation of friable solids thereby increasing the surface area, 3) High-velocity interparticle collision in slurries and 4) surface damage at liquid-solid interfaces by microjets and shock waves.

A feature that can occur during collapse of cavitation bubbles in liquid systems is the development of re-entrant jets. The presence of a solid interface adjacent to a cavitation bubble can cause an asymmetrical collapse resulting in a microjet. This is an important factor for the damage of materials, as most of the energy of the microjet is directed at the solid-liquid interface. In Figure 2 a photograph of the formation of a microjet illustrates how the energy of a jet is directed towards the solid-liquid interface[11].

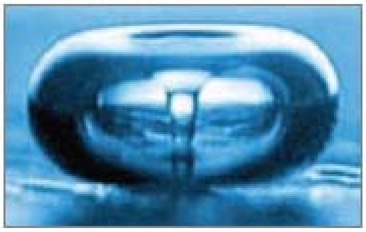

Figure 2: A photograph of the formation of a microjet[9].

Kolyer's Aluminium foil Erosion test

In 1988, John M. Kolyer devised a method to characterize the energy distribution of ultrasonic baths by using the erosion of aluminium (pitting) foil that is caused by microjets. By placing strips of foil in an ultrasonic bath and measuring the weight before and after sonication the erosion is quantified[12, 13].

To find out if cavitation was present in our ultrasonic tank, an aluminium foil erosion test was done. Three narrow strips (approx. 10x50 mm) of Labor™ (0.030 mm thick) aluminium foil were cut (Figure 3). Two of these were put in separate Fliofax test tubes and 20.0 ± 0.1 ml of demi water was added. The test tubes were submerged in the ultrasonic bath and the third strip of aluminium was freely suspended in the ultrasonic tank (without test tube). The three strips were exposed to ultrasound for five minutes. By weighing the strips before (b) and after (a) sonication, a simple measurement for erosion (*f*) was established.

The weights of the strips were carefully documented. There was about 25% weight loss due to erosion in a 5 minute sonication period (Table 1). The erosion was established with the following equation:

$$f = \frac{m^b - m^a}{m^b} \qquad <1.1>$$

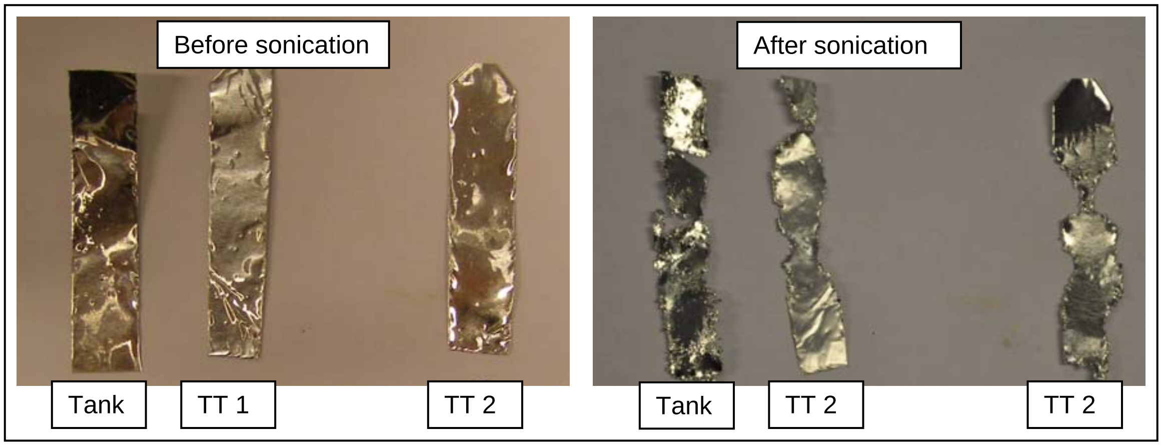

Figure 3: Pictures of the Aluminium Foil Erosion test. The strips are approxemately 10x50 mm and 0.030 mm thick, initially.

Table 1: The weight of the strips before (*b*) and after (*a*) sonication and the weight fraction that was lost due to erosion (*f*).

	Tank	**TT1**	**TT2**
m^{b} *[g]*	0.0517	0.0461	0.0499
m^{a} *[g]*	0.0384	0.0334	0.0389
f [-]	0.26	0.28	0.22

2.4. Experimental setup and results

A method was developed to test the effect of acoustic stimulation on the dissolution of sodium chloride salt (NaCl) in water. Twelve (12) Fliofax® 20x180 mm test tubes with beaded rim were used. These were filled with *10 ± 0.1 g* of salt and *20 ± 0.1 ml* of demineralised water. By first pouring in and levelling the salt and then carefully filling demineralised water with a 230 mm long glass Pasteur pipette (WWR-International™) only a minimal amount of salt was dissolved in the water. It is to be expected that the salt will gradually dissolve in water.

To speed up the dissolution process, the test tubes were mounted in a tray and immersed in a water filled 44 kHz ± 6% ultrasonic bath (Bransonic® B-8510E DTH). The open upper end of the tube remained above the water level of the ultrasonic tank (see Figure 4).

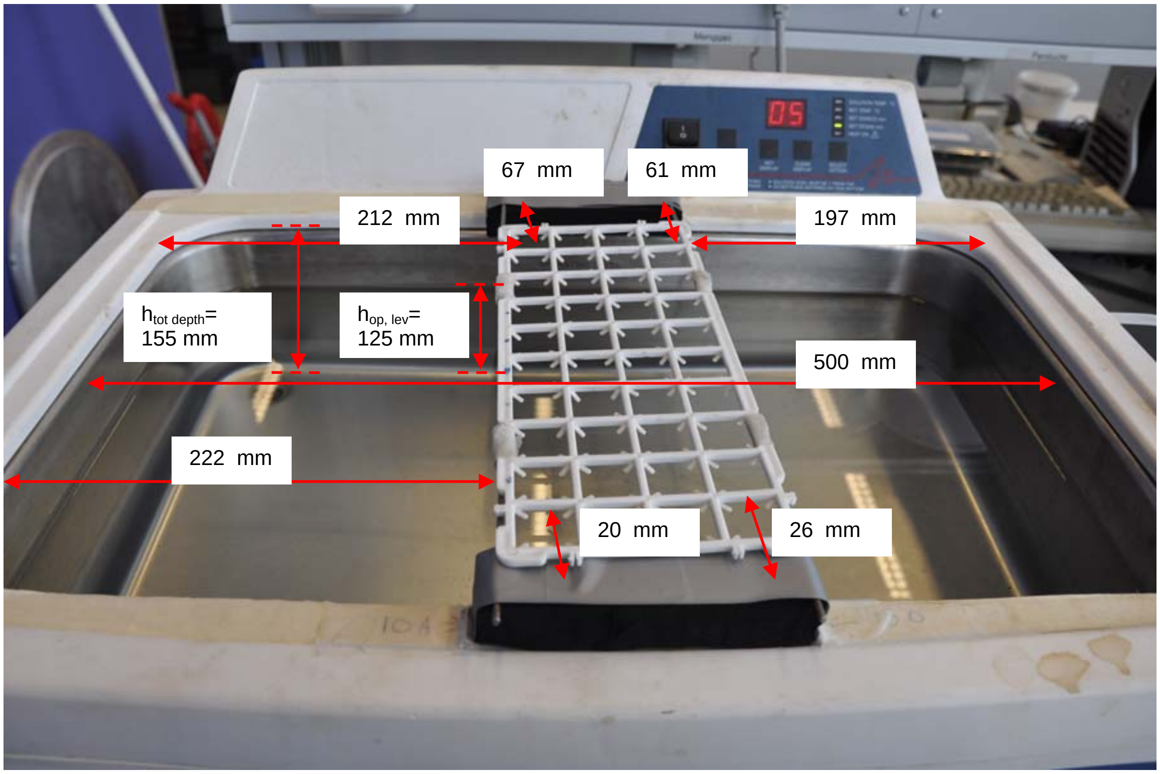

Figure 4 : Set up. The distance from the top of the test tube (=top of tray) to the bottom of the tank is 185 mm ± 0.5 mm and the total length of the test tube is 180 mm. This means that the gap between the tank and test tube is 5 mm ± 0.5 mm. The tray (test tube holder) is visible in the centre on top of the foam blocks.

The ultrasonic tank was then operated for five minutes at operational intensity (250 W HF- output). There was a significant amount of salt dissolved in water after sonication. The volume decrease (expressed as $\Delta h = h^b - h^a$) of the solid phase was measured by marking the height of the solid phase with a waterproof marker before sonication. After sonication the difference between the marking and the new salt level (Δh) was measured with a (standard) ruler.

The experiment was repeated three times under identical circumstances and Δh was recorded. An overview is given in Table 2 (the three colours relate to the three experiments). The data are also plotted in Figure 7.

Most of the test tubes had horizontal salt levels after sonication. A few however had slanted salt levels (Bold notations in Table 2). The new salt level was calculated by linear interpolation: $h_{avg}^a = (h_{max}^a + h_{min}^a)/2$ (see Figure 6 for schematic drawing). These points were considered to have a higher experimental error ($\varepsilon = \pm(h_{max}^a - h_{min}^a)/2$) than the data where the salt level remained horizontal (see Table 2).

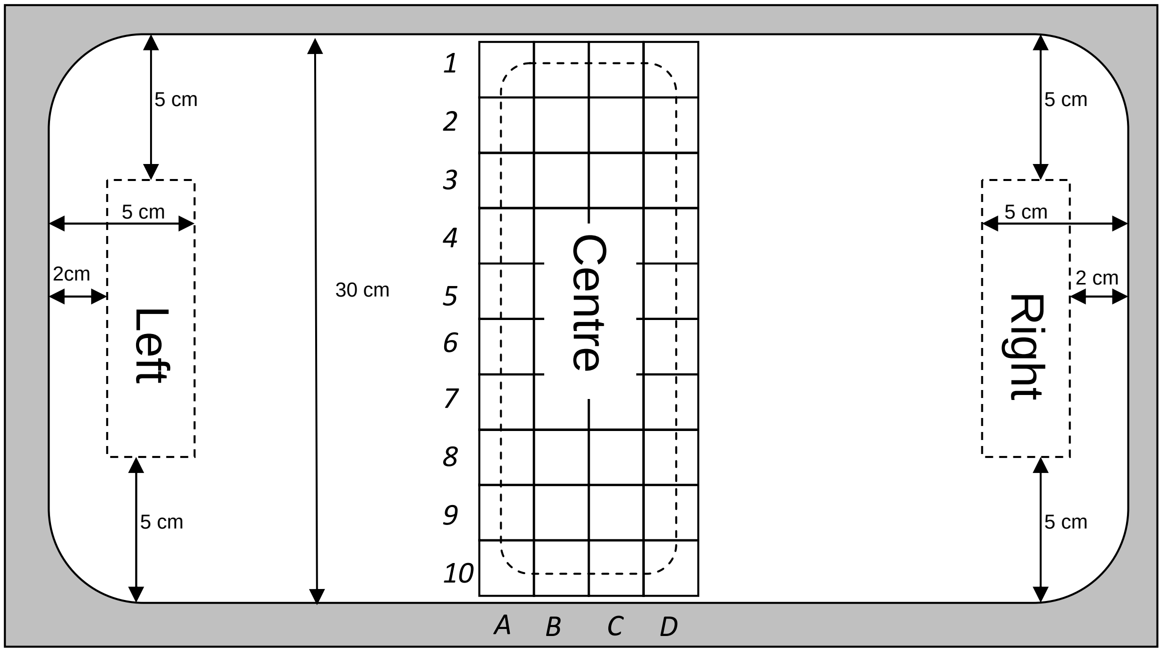

Figure 5: Schematic representation of the acoustic bath. The temperature was measured in the left, right and centre boxes.

Table 2: Drop in salt level, Δh after 5 min sonication. The bold entries had a slanted salt level after sonication and a higher uncertainty (as explained below). The rows (1-9) and the columns (A-D) in the table coincide with the rows and columns of the test tube tray. [exp. 1= green, exp2 = pink, exp 3 = blue]

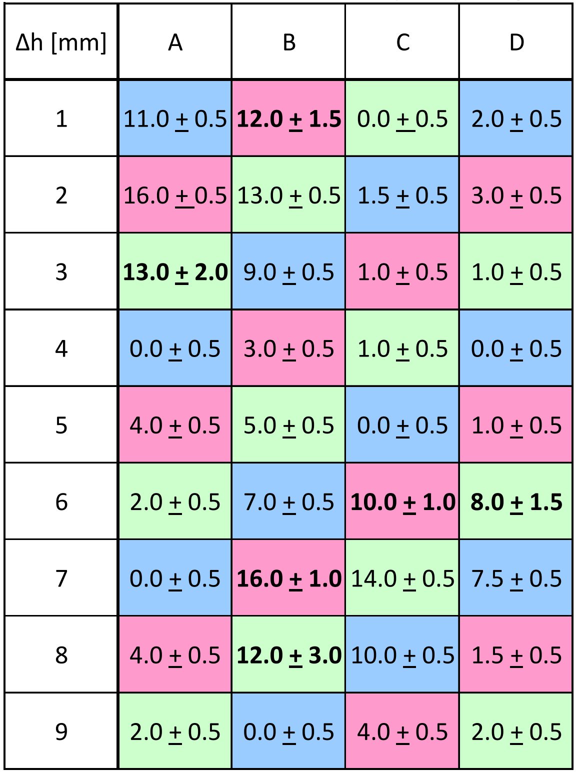

Δh [mm]	A	B	C	D
1	11.0 ± 0.5	**12.0 ± 1.5**	0.0 ± 0.5	2.0 ± 0.5
2	16.0 ± 0.5	13.0 ± 0.5	1.5 ± 0.5	3.0 ± 0.5
3	**13.0 ± 2.0**	9.0 ± 0.5	1.0 ± 0.5	1.0 ± 0.5
4	0.0 ± 0.5	3.0 ± 0.5	1.0 ± 0.5	0.0 ± 0.5
5	4.0 ± 0.5	5.0 ± 0.5	0.0 ± 0.5	1.0 ± 0.5
6	2.0 ± 0.5	7.0 ± 0.5	**10.0 ± 1.0**	**8.0 ± 1.5**
7	0.0 ± 0.5	**16.0 ± 1.0**	14.0 ± 0.5	7.5 ± 0.5
8	4.0 ± 0.5	**12.0 ± 3.0**	10.0 ± 0.5	1.5 ± 0.5
9	2.0 ± 0.5	0.0 ± 0.5	4.0 ± 0.5	2.0 ± 0.5

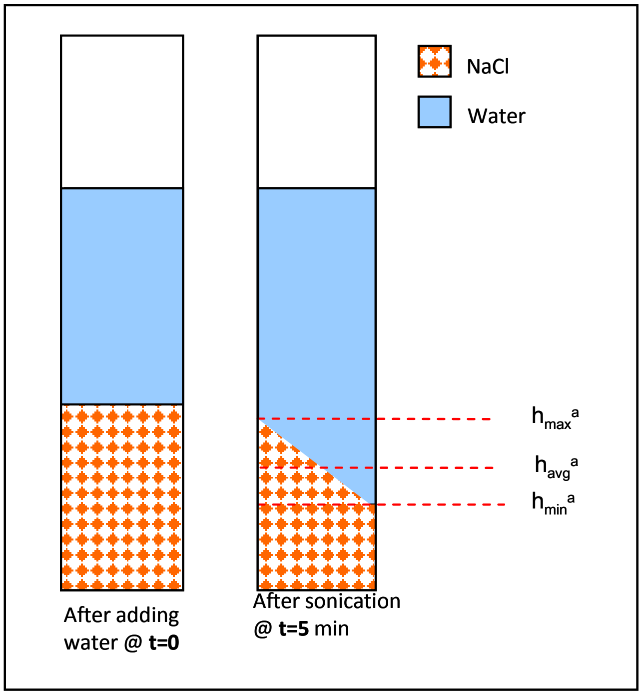

Figure 6: Schematic drawing of tilted salt level.

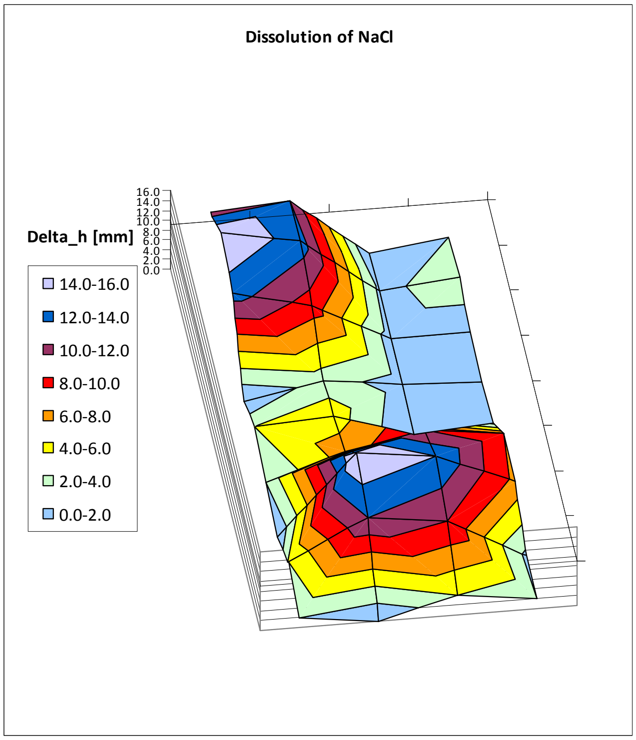

Figure 7: Results of the experiment. The horizontal plan has coordinate points that coincide with the tray used in the experiment (Figure 4). The vertical axis depicts the drop of salt (in [mm]) after a five minute sonication period.

Control experiment

Of course, dissolution also takes place in the absence of ultrasound (natural dissolution). To measure dissolution enhancement by sonication, a control experiment was performed. The control was performed on a single test-tube. The test tube was left out of the ultrasonic bath and the dissolution was measured regularly. The salt level typically dropped 3.5 ± 0.5 mm over 20 hrs (Figure 8). It can be noted that the average dissolution of salt over the 5 mins sonication period is 5.5 mm, which is more than the natural dissolution over a 20 hrs time span. It can be noted that dissolution is enhanced considerably by acoustic sonication. As the natural dissolution of the salt takes place on a much longer timescale, the acoustic simulation may be assumed a “frozen” experiment.

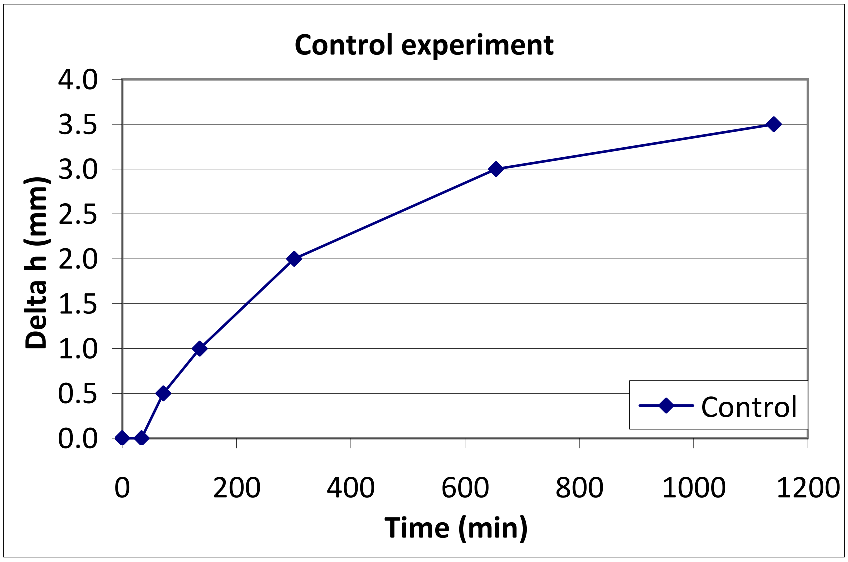

Figure 8: Control experiment. No acoustic stimulation.

Temperature effect

The temperature of the tank could also have an effect on the dissolution process. The temperature was therefore recorded by means of a Voltcraft k102 digital thermometer. An empty tank was sonicated and the temperature was measured and recorded regularly in three separate areas (see Figure 5 for details) within the bath. The results suggest that the temperature increase within the tank due to sonication is independent (see Figure 9) of the location. It is likely that the temperature is homogenized by mixing.

From the literature the solubility of NaCl in water is found to be temperature dependant (Figure 10). As the temperature variations are small, so will the change in solubility.

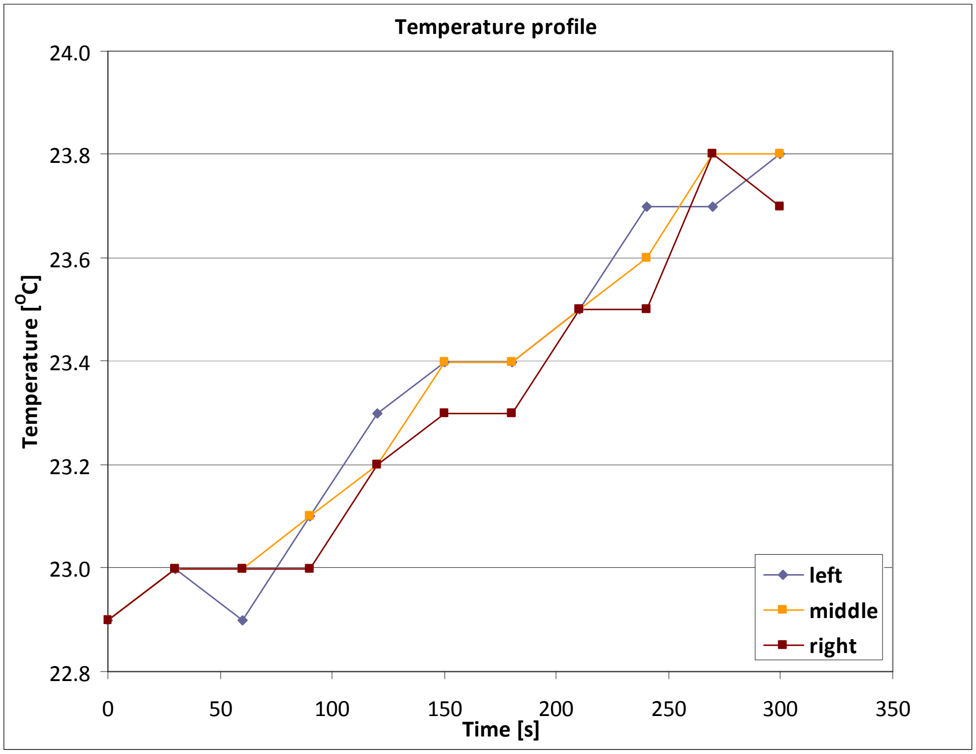

Figure 9: Temperature recordings in different locations (Figure 5) of the tank.

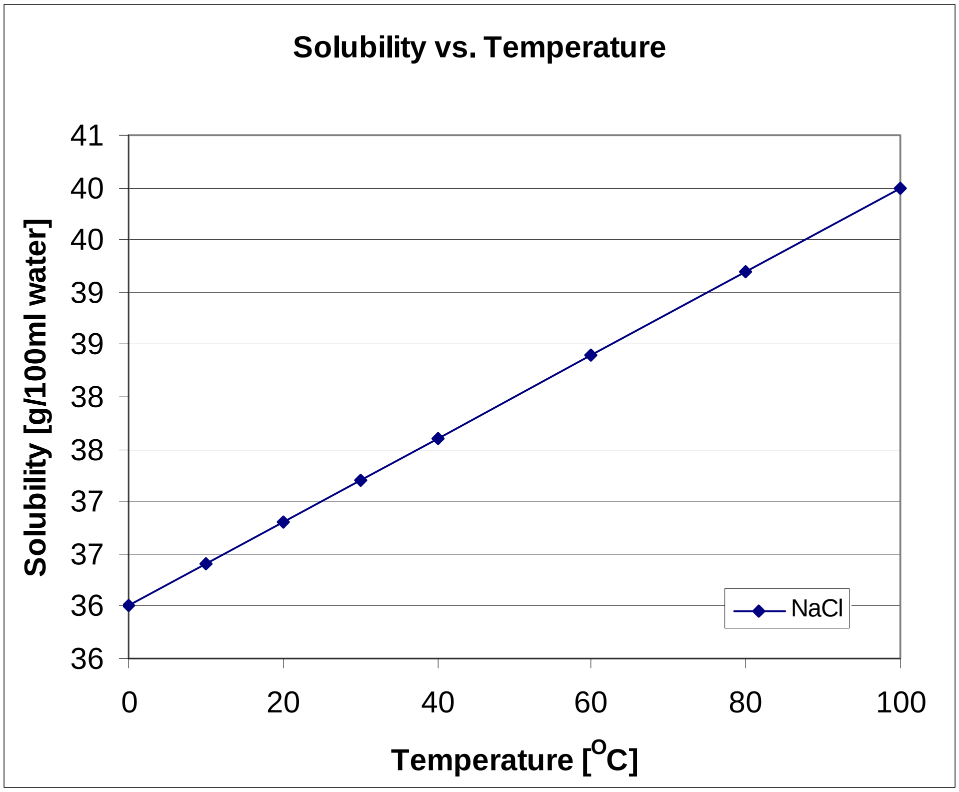

Figure 10: Solubility data[14].

Dissociation experiment

To relate the measured drop in salt level to dissolution another control experiment was set up. Ions increase the conductivity of the solvent. By measuring the conductivity of the solvent before and after sonication a measure for dissociation was established.

Two test tubes were filled with the same quantities of both salt and water (20.0 ± 0.1 ml of demineralised water and 10.0 g ± 0.1g of NaCl) as in the previous experiment. The conductivity was measured with an electrical conductivity meter (WTW Multi 340i with a Tetracon^{tm} 325 electrode) before and after treatment. The sonication lasted for five minutes and the test tubes were treated simultaneously.

As a reference a saturated solution was prepared. A test tube was filled with *20.0 g ± 0.1 ml* of demineralised water and *10.0 g ± 0.1 g* of NaCl. It was shaken vigorously by hand for five minutes. Afterwards the test tubes were left in a test tube holder for 15 min. It was assumed that this was enough time for precipitation. After 15 min the *Δh* and the conductivity were measured and registered.

As the solubility of sodium chloride in water is ± 37 g/100 ml (@atmospheric pressure and 25°C, see Figure 10), an amount of salt will not dissolve and can be recognized as a separate phase at the bottom of the test-tube. This experiment gives an upper limit for conductivity and the salt level.

Results -Dissociation experiment

When measuring the conductivities of the three different solutions it was observed that the first measurement was unexpectedly low. When the measurement was repeated, it was significantly higher than the first measurement. It could be concluded that the salinity of the solvent was not homogeneous throughout the test tube.

It was observed that an interface was present within the solvent. It is likely that the interface was due to a high salt concentration gradient. A transparent interface could be seen within the solvent. Inserting the electrode of the electro-conductivity-meter into the test tube agitated the interface. It is likely that this was the cause of the inconsistent readings of the conductivity.

After letting the test tubes rest for 20 hrs, the interface was not visible anymore. When the electrode was inserted a couple of times however, the same inconsistent conductivities were measured. This suggests that the high salinity gradient was still present.

It was concluded that the conductivities that were measured are probably not good for quantitative data analysis. The significant increase in overall conductivity does suggest however that a significant amount of solid phase has dissociated. To give an impression, the highest conductivities measured were registered in Table 3.

For the reference table, the total measured drop in height was 18 mm ± 0.5 mm. Furthermore, the conductivity was measured at 242 mS/cm (see Table 3). These readings were more or less consistent (± 1 mS/cm), indicating that the vigorous shaking creates a homogeneous salt solution where as the ultrasound treated test tubes does not.

Table 3: The conductivity of the two test tubes before sonication and 20 hrs after a 5 minute sonication period. Furthermore the values for the saturated solution are given. The highest recorded conductivity values are given.

	test tube 1		test tube 2	
	Conductivity	delta h	Conductivity	delta h
	mS/cm	[cm]	mS/cm	[cm]
demineralised	3.00E-03	[-]	3.00E-03	[-]
Before sonication	9.98	<1	11.2	<1
after 20 hrs	55.02	9	65.7	10
	saturated			
	Conductivity	delta h		
	mS/cm	[cm]		
5 min shaking	244	18		

2.5. Discussion

Salt dissolves significantly faster when treated with ultrasound. In the experiment, the sonicated test tube showed a larger decrease in salt level after a five-minute sonication period than the untreated control tube did after 20 hrs. Furthermore, the dissolution rate within the test tubes proved to be position dependent within the ultrasonic bath. The difference in Δh that was observed between different locations was sometimes 16 mm. This could make the dissolution of salt a viable method for characterizing the energy distribution of an ultrasonic bath.

In addition, it is important to note that some of the salt levels were slanted after sonication with respect to the initial horizontal condition. The reason for this is that the test tubes were probably situated at a sharp intensity boundary. The fact that there was a difference in salt level within a single test tube suggests: a) there was a sharp gradient between high and low intensity regions within the bath (Figure 7). b) The salt dissolution method is sensitive enough to capture a sharp energy gradient if it were to be used to characterize the energy distribution of an ultrasonic bath.

3. The Effect of ultrasound on the emulsification of hexadecane, water and alpha-olefin-sulphonate

3.1 Abstract

Ultrasound was used to emulsify hexadecane and a water-surfactant solution. The goal was to study the effect of surfactant concentration on the formation of a middle substance (emulsion or other). Additionally the composition and structure of the resulting middle layers were analyzed.

Test tubes filled with a water phase (demineralised water and alpha-olefin-sulphonate surfactant) and hexadecane (oil) were placed in an ultrasonic tank. Next the tubes were exposed to ultrasound for 30 min. Over the range of surfactant concentrations that have been tested (0.05–46wt %) all the test tubes formed a middle substance after sonication. The surfactant concentration appeared to have an influence on the type of middle substance that formed after sonication as well as the quantity of the middle substance.

The quantities of middle substance that formed during the 30 min sonication varied from 0.8g (@ 44wt% initial surfactant concentration) to 8.7g (@ 4wt% initial surfactant concentration).

Two different middle substances could be distinguished: An opaque, whitish o/w emulsion and a translucent, amber coloured semi-solid gel-like material. From a thermogravimetric analysis (TGA) it was likely that the latter had low (± 5%) oil content. Furthermore the structure of the gel has been analyzed with a scanning electron microscope (SEM). The results of the SEM showed that the structure of the gel contained two types of porosity with two orders of magnitude. The largest is spherical in shape and 50 - 500 µm in diameter. The smaller pore type are found in the matrix of the gel. They are wormhole-like shapes and are 1 - 3 µm in diameter.

Keywords
[Oil-in-water-emulsions, gel, ultrasound, SEM, TGA, refractive index]

Nomenclature

Δm	*Decrease in weight*	*[g]*
m	*Total mass of middle substance*	*[g]*
m_1	*Mass of upper layer*	*[g]*
m_2	*Mass of lower layer*	*[g]*
ε	*Experimental error of mass*	*[g]*
error	*Experimental error of mass fraction of the middle phase*	*[-]*
γ	*Mass fraction of surfactant in lower layer*	*[-]*
γ_O	*Mass fraction of oil in middle substance*	*[-]*
γ_W	*Mass fraction of water in middle substance*	*[-]*
γ_S	*Mass fraction of surfactant in middle substance*	*[-]*
m_O	*Mass oil in middle substance*	*[g]*
m_W	*Mass water in middle substance*	*[g]*
m_S	*Mass surfactant in middle substance*	*[g]*
O	*Oil*	*[-]*
W	*Water*	*[-]*
S	*Surfactant*	*[-]*
1	*Upper layer*	*[-]*
2	*Lower layer*	*[-]*
b	*Before sonication*	*[-]*
a	*After sonication*	*[-]*

3.2 Introduction

Emulsions have many of applications in a wide range of industries. Amongst them we identify the food industry (milk, butter), the cosmetics industry (lipstick, shampoo) and the pharmaceutical industry (ointments, artificial blood substitute). But also in the oil industry there are numerous important applications. Emulsions are used, for instance[6] for mobility control where increasing the mobility can improve the recovery of a reservoir. But emulsions are also used for decreasing the mobility. By decreasing the flow in high permeable thief zones, the sweep of the reservoir can be increased[15].

An emulsion is a dispersion of two immiscible fluids. It is inherently unstable and does not form spontaneously. With the input of energy it is possible to disperse one liquid (dispersed phase) into the other (continuous phase). Over time, due to the kinetic instability, the liquids return to their separated phases (Figure 11*c*). By introducing a surfactant it is possible to create a stable or meta-stable emulsion. The dispersed phase is typically distributed as droplets (see Figure 11)[15].

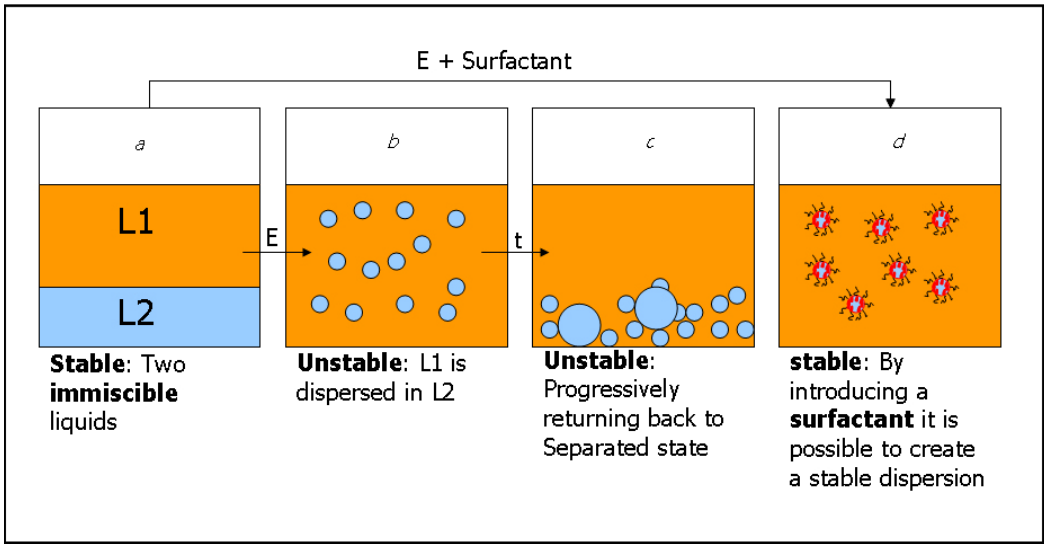

Figure 11: From left to right schematic drawings of: *a)* two immiscible liquids, *b)* with the input of energy it is possible to create an unstable emulsion, *c)* After some time the liquids will return back to a stable situation (*a*), *d)* It is possible to create a stable emulsion when also a surfactant is added in addition to energy. Micelles are created consisting of stable droplets.

The most common surfactants have a similar basic chemical structure: their molecule is formed by a hydrophilic (water loving) head and a hydrophobic (water fearing) tail[16]. Due to strong interaction with water molecules, surfactants are water soluble. Due to the amphiphilic② nature of the molecule it is favourable for surfactants to reside at interfaces. This characteristic of the surfactant molecule is the driving force behind the formation of micelles. Micelles are dynamically stable droplets where, depending on what the continuous/ dispersed phase is, the tail sits in one phase and the hydrophilic head in the other[17].

There are many systems that can create emulsions. An example of such a system is the rotor-stator-stirring system: the turbulent flow that results from the rotor creates shearing forces enabling the mixing of two liquids. It is also possible to disperse oil and water with ultrasonic waves[18].

Dispersing one liquid into another via ultrasound is most likely caused by instable (transient) cavitation (explanation in chapter 1) and the associated phenomena, such as microjets and turbulent flow[19,20,21,22].

The goal of this experimental study is to document the effect of ultrasound on oil-water systems for varying surfactant concentrations. Additionally the composition and structure of the resulting middle substances were analyzed and discussed.

3.3 Experiment

Materials and Methods

For generating acoustic energy a 250 W (HF- output), 44 ± 6% kHz Bransonic® B-8510E DTH ultrasonic bath was used. The bath has a significant heterogeneous acoustic

---

② Amphiphilic: A chemical compound possessing both hydrophilic as lipophilic properties.

energy distribution. To characterize this distribution an experiment was set up, as explained in chapter 1.

The surfactant used to carry out the experiment is: alpha-olefin-sulphonate (AOS) AS 1246 (Stepantan^{TM}, batch# 7228230). This is an industrial-grade surfactant commonly used in the oil industry for (amongst other applications) enhanced oil recovery (EOR). The surfactant solution contained 46.6% solids, of which 46.3 wt% are active ingredients. The active components are: 1-dodecanesulfonic acid, hydroxy-sodium salt (10 –30%) and dodecene-1-suldonic acid sodium salt (20 –30%) [see Appendix A: Manufacturers datasheet].

The oil used was n-hexadecane with 99% purity manufactured by Sigma-Aldrich Company.

Experimental setup

The ultrasonic bath was used as emulsification system. A description is given in chapter 1. By mounting two test tubes in a test tube tray and placing the tray over the ultrasonic bath the test tubes are partly immersed and exposed to ultrasound (Figure 12). The test tubes were sonicated for 30 minutes. The test tubes had identical initial conditions. (based on experimental data from chapter 1, coordinate A and B Figure 12). All test tubes, exposed to ultrasound contained 5.0 ± 0.1 g of oil and 5.0 ± 0.1 g of demineralised water to which surfactant was added (Table 4). The top of the test tubes (Fliofax® 20x180 mm with beaded rim) were open and kept above the surface of the water of the ultrasonic tank. After the 30 min sonication the test tubes were left to rest for half an hour after which they were taken out of the bath and photographed.

As it was conceivable that the temperature would have a significant impact on the results, the water in the ultrasonic tank, which would heat up 5.5^{O}C on average (based on results from Table 4) after 30 min. of sonication, was removed and refreshed after every experiment. The temperature was measured before and after sonication (Table 4).

Remarkably all the test tubes had developed a distinct layer in between the oil on top and the water beneath. It was identified as either a gel or as an emulsion. This will be discussed in the forthcoming.

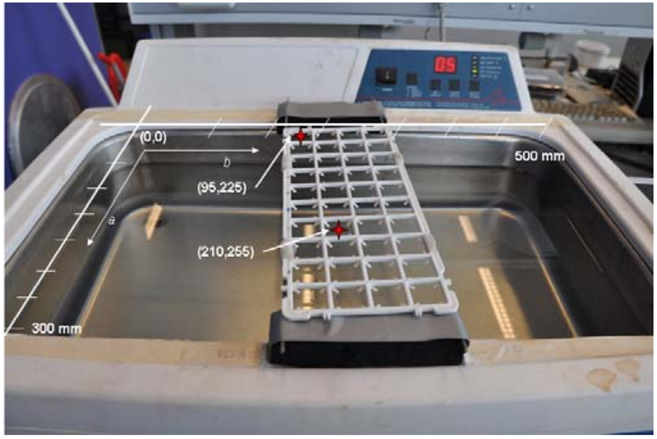

Figure 12: Setup of experiment with the two high energy regimes where test tubes were placed are marked. Coordinates are given in mm and are expressed as (*a*,*b*).

Table 4: Quantities of lower (2)- and upper (1) layer that was present in every experiment. The surfactant (AOS, Stepan, AS-1246) water mixture (γ) was obtained by diluting the surfactant solution. The temperatures (T) of the solution before (b) and after (a) sonication are also given.

Coord	Y^b	m_2^b	m_1^b	T^b	T^a
[-]	[-]	[g]	[g]	[^{O}C]	[^{O}C]
B	5.0E-04	4.9	5.1	21.4	26.5
A		5.0	4.7		
B	1.0E-03	5.0	4.9	20.4	25.6
A		5.0	4.7		
B	1.0E-02	4.9	4.9	20.6	26.1
A		5.0	4.9		
B	2.0E-02	5.1	5.1	21.2	27.6
A		5.0	5.0		
B	0.04	5.0	4.9	20.1	25.2
A		4.9	4.9		
B	0.08	5.1	4.9	22.8	28.0
A		5.0	4.9		
B	0.12	5.0	5.0	22.5	28.0
A		4.9	5.1		
B	0.16	5.0	4.9	20.0	26.4
A		5.0	5.1		
B	0.20	5.0	5.1	21.1	26.0
A		5.1	4.9		
B	0.24	5.0	4.9	22.0	27.5
A		5.0	5.1		
B	0.28	5.0	5.0	21.4	26.9
A		5.0	4.9		
B	0.32	4.9	5.1	22.7	27.7
A		5.0	5.0		
B	0.36	5.0	5.0	19.6	25.5
A		5.0	5.1		
B	0.40	4.9	5.0	19.8	25.6
A		5.0	4.9		
B	0.44	5.0	5.1	21.6	26.6
A		5.0	5.0		
B	0.46	4.9	5.0	19.7	25.8
A		5.0	5.1		

Experimental procedure for preparing the water-surfactant mixture

The surfactant solution, of 46 wt% active ingredient, was diluted with demineralized water. For this a scale (SI-234 Denver Instruments^{TM} , ± 0.1 mg) was used. In this fashion the surfactant solution was diluted to 16 different concentrations (from 0.05 wt% to 46 wt%, Table 4). The solution was homogenized by mixing with a magnetic stirrer for approximately three minutes. The surfactant solution was then placed in the test tube using a pipette. The surfactant solution had a greater density than hexadecane (> 1 g/cc with respect to 0.773 g/cc of hexadecane) it was placed first to prevent mixing prior to sonication. Special care was taken to prevent the glass surface above the water phase interface from being contaminated with the solution during filling (see Figure 13). By filling the test tube with a pipette that was long enough to reach the bottom this undesired effect could be avoided. In order to create a stable bimodal layer, the hexadecane was carefully added on top of the surfactant solution. In this case special care was taken as not to disturb the oil phase-water phase interface. This was done by letting the hexadecane flow along the glass surface of the test tube. If the precaution was not taken and the hexadecane would be poured directly onto the surfactant solution interface the oil and water phase would sometimes emulsify prior to sonication (see Figure 13).

Next the tubes were sonicated (30 min) as previously discussed.

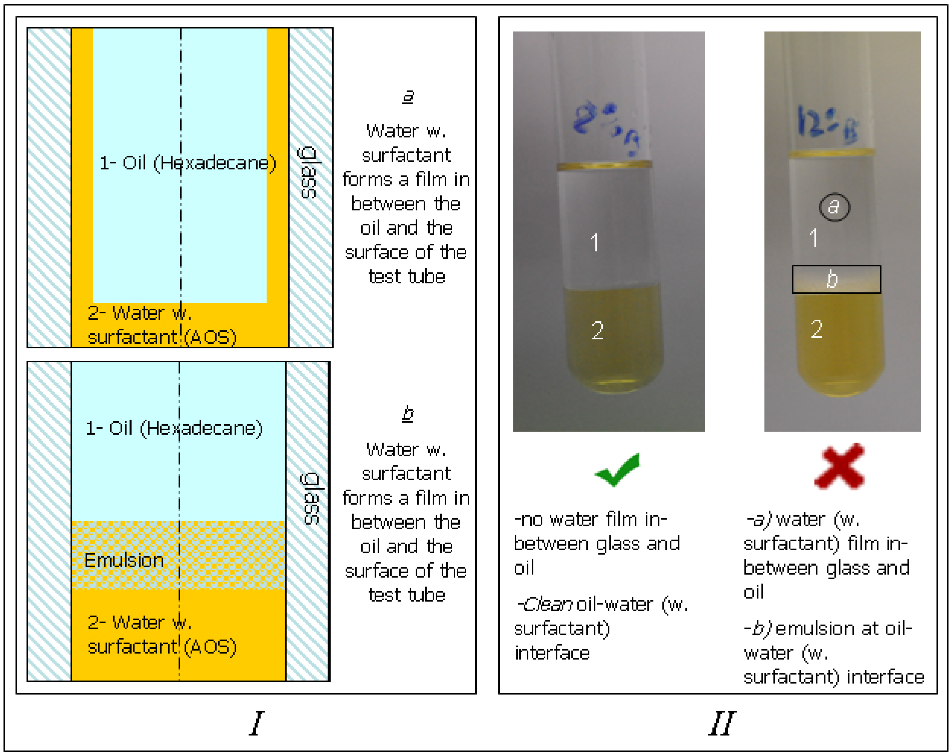

Figure 13I & II: Pictures of two prepared test tubes. The schematic drawings as well as the pictures depict what could happen if the correct precautions are not taken when filling the test tube (*a* and *b*). *a*) The water phase forms a film between glass surface and oil phase. *b)* Oil and water phase have formed an emulsion prior to sonication

3.4 Results

Phase behaviour of the middle phase

After sonication the test tubes that were removed from the ultrasonic bath and left out in the open for four days. Over the 4 day period the upper layer (hexadecane) within the test tubes, which had a semi-translucent whitish appearance turned translucent. The result can be observed in Figure 14. After this period the test tubes were photographed again (Figure 15).

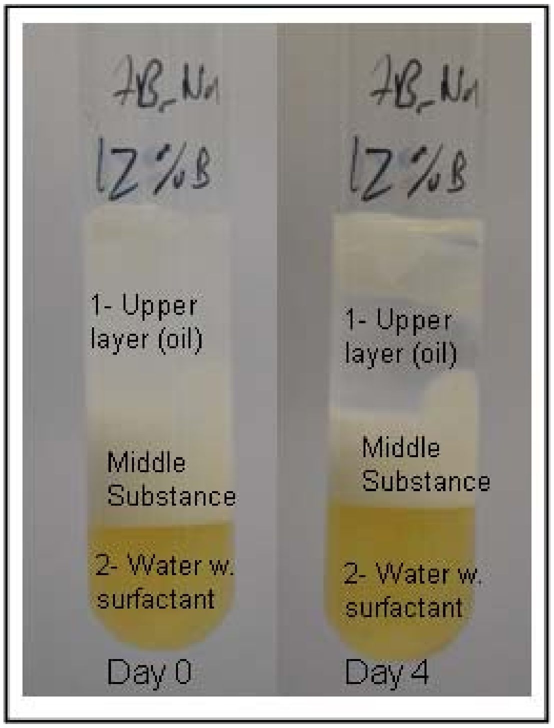

Figure 14: The oil phase has a white opaque hue directly after sonication. After a four day period the oil takes on a comparable translucent colouring as to before sonication. The example is of 12 wt% initial surfactant concentration.

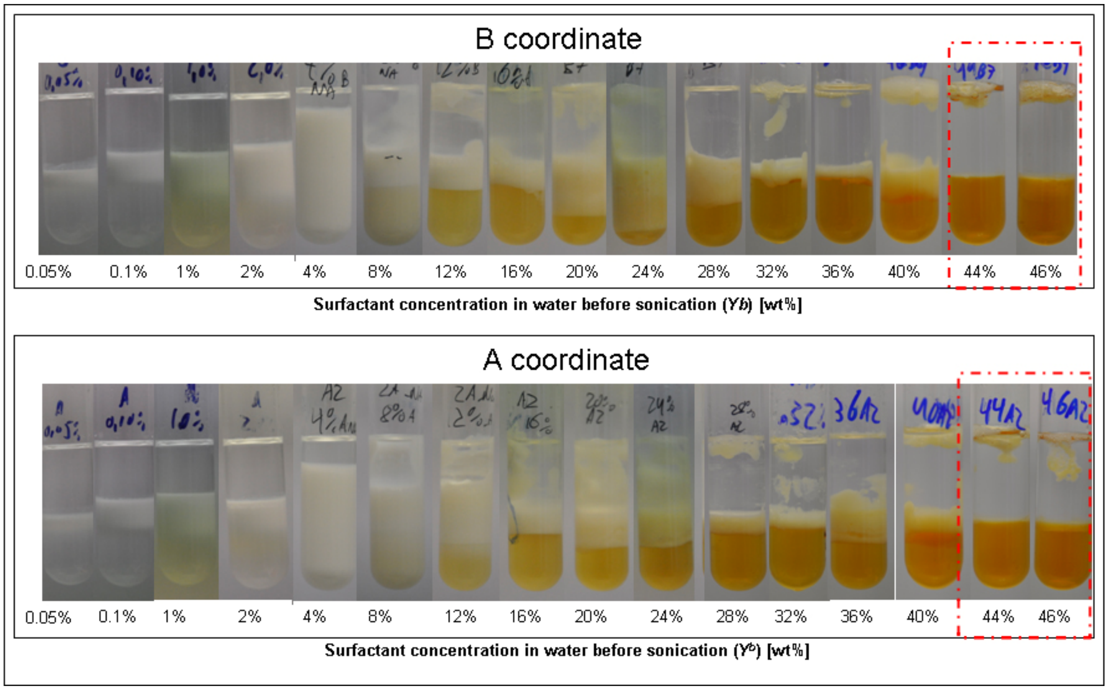

Figure 15: Photographs of test tubes after sonication. The test tubes labelled after the initial surfactant (AOS) wt% in the surfactant solution. At an initial surfactant concentration 4 wt% it can be observed that the water phase is no longer present and that a maximum of middle substance is present. The red box identifies the test tubes with a gel like middle substance.

It was observed that after the 30 min sonication period every treated test tube contained a new substance in between the oil and surfactant solution. All the middle substances formed over the entire diameter of the test tube. Most of these substances were an opaque, white-yellowish coloured emulsions in between the oil and surfactant solution. With a standard dilution experiment the emulsions have all been identified as oil-in-water emulsions (o/w). By slowly adding water (the dilutant) to the emulsion a quick identification can be made of the emulsion. When the emulsion forms a separate phase to the dilutant, the continuous phase was identified as oil (w/o). When the emulsion was diluted by the water, the continuous phase was identified as water (o/w)[23].

Another point of interest was that from Figure 15 it could be seen that the amount of emulsion that was produced appeared to have a maximum at 4 wt% surfactant (initial surfactant concentration of the water phase). At 4 wt% initial surfactant concentration, the surfactant solution was no longer present after sonication.

An explanation for this could be that: an increase in surfactant concentration lowers the interfacial tension therefore it can be expected that the activation energy required to create the emulsion is lower. Thus for a higher surfactant concentration an increase in middle substance volume is expected. The amount of middle substance that was formed decreased at after a certain increase in surfactant concentration. This could be explained when the viscosity is taken into account (depending on the surfactant concentration ranging from 1 cP to 160 cP @ 25 ^{0}C). As the viscous forces start to dominate, turbulent mixing is less vigorous and this will result in the formation of less middle substance.

In some cases the middle substance was identified as a translucent amber-coloured, semi-solid material (Figure 16). This particular middle substance formed at an initial surfactant concentration of 44–46 wt% (Figure 15). It is now referred to as a gel. Both the emulsion as well as the gel middle substance have remained stable for the duration of the study (>4 months).

Figure 16: Picture of the gel removed from the test tube. The diameter of the gel is approximately the same as the test tube (20 mm).

The gel proved difficult to be removed from the test tube. It had a sticky, solid like rheology that adhered readily to the glass surface of the test tube. The stability and previously mentioned properties could make the gel a suitable agent for mobility control. Extra attention was therefore given to the gel. Different methods have been used to describe:

All middle substances:

- By weighing the oil and the water with surfactant mixture before and after sonication it is possible to set up a mass balance. For quality control of the calculation an uncertainty analysis was done.

Gel-like middle substances:

- Thermogravimetric analysis (TGA) was used to quantify the mass fractions of the three components (oil, water and surfactant) in the middle substance. As this method is relatively time consuming only the gel was analyzed with TGA.
- Optical analysis with the Philips^{TM} XL20 scanning electron microscope (SEM). By first freeze-drying (removing the continuous phase, see Figure 17) a gel sample it is possible to observe the structure of the gel with the SEM.

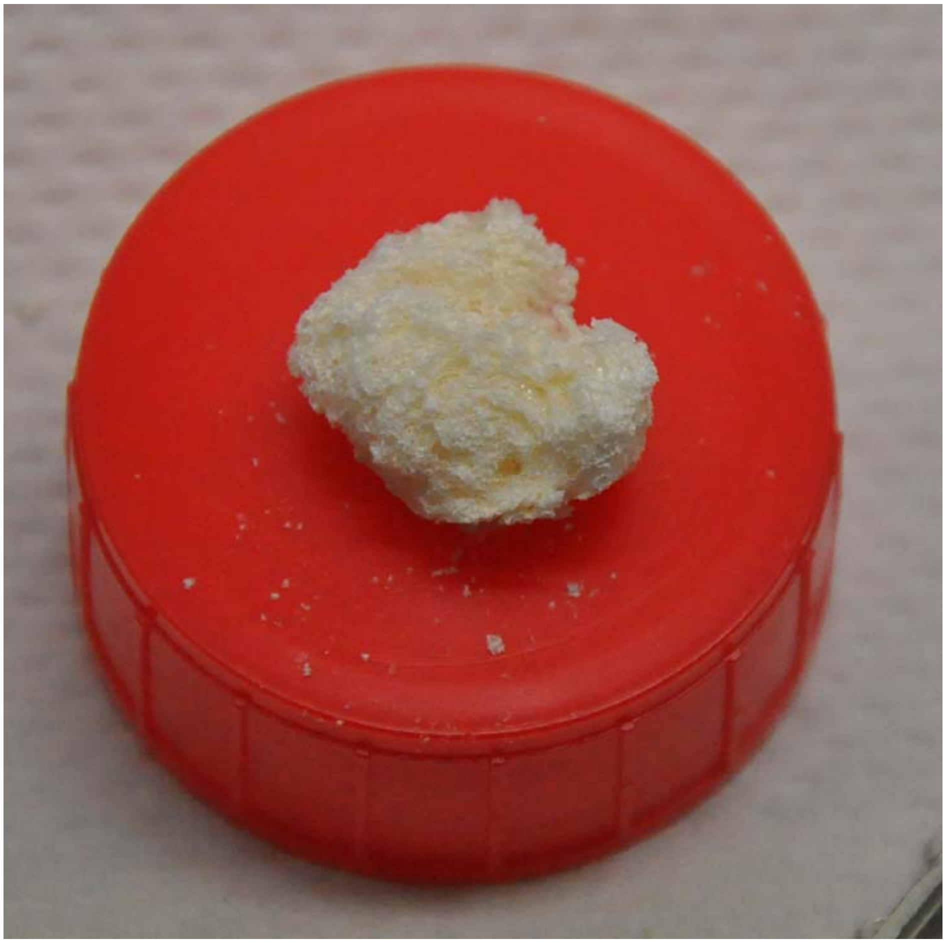

Figure 17: Picture of the gel after freeze drying. The red cap is approximately 4 cm in diameter.

Quantitative analysis of the middle substance

An objective of the experiments was to quantify the new formed layer in terms of oil (*O*), water (*W*) and surfactant (*S*) in terms of mass (*m*). The individual mass components can be expressed as:

$$\begin{aligned} m_O &= \Delta m_1, \\ m_w &= \Delta m_{W2}, \\ m_S &= \Delta m_{S2}. \end{aligned} \tag{2.1}$$

The lower layer (2) consists of water and surfactant. This means the quantities before (*b*) and after (*a*) sonication could be related:

$$\Delta m_{W2} = (1-\gamma^b)m_2^b - (1-\gamma^a)m_2^a, \tag{2.2}$$

$$\Delta m_{S2} = \gamma^b m_2^b - \gamma^a m_2^a \tag{2.3}$$

Adding equations 2.2 and 2.3 it is found for the new layer:

$$\begin{aligned} m_O &= \Delta m_1, \\ m_w + m_S &= \Delta m_2, \end{aligned} \tag{2.4}$$

Which also means that the total mass in the new layer is given by $m = m_O + m_W + m_S = \Delta m_2 + \Delta m_1$. The mass fractions of the components in the layer are defined as follows:

$$\begin{aligned} \gamma_O &= \frac{\Delta m_1}{\Delta m_1 + \Delta m_2}, \\ \gamma_S &= \frac{\gamma^b m_2^b - \gamma^a m_2^a}{\Delta m_1 + \Delta m_2}, \\ \gamma_W &= 1 - \gamma_O - \gamma_S. \end{aligned} \tag{2.5}$$

The quantities of oil (m^b_1) and surfactant solution (m^b_2) before sonication were carefully weighed and registered. The mass fraction of surfactant in the lower layer before sonication (γ^b) was also known.

The mass of these phases were calculated by removing the phases with a syringe and weighing mass of the test tube before and after extraction. The only unknown, necessary to calculate the mass fraction of the three components within the middle substance, was the concentration surfactant (γ) in the lower layer (*2*) after sonication (*a*).

Table 5: Table with all the measured and calculated masses (*m*) of the three components water (*W*), *oil* (*O*) and surfactant (*S*) for both the upper (1) as well as the lower (2) layer before (*b*) and after (*a*) sonication. The masses as well as the mass fractions (γ) of the middle substance (without layer subscript) were calculated with the mass balance as described in the previous paragraph. Authors' note: The *γ* (w. subscript O, W and S) in the last three columns are in latter paragraphs referred to as γ^{ε} (w. subscript O, W and S). The abbreviation NP stands for *not present* and means that no measurable amount of the specific layer was present after sonication.

Coord	**before sonication**			**after sonication**									
name	m_1^b	m_2^b	γ_2^b	m_1^a	m_2^a	γ_2^a	m_O	m_W	m_S	m	γ_O	γ_w	γ_s
[-]	[g]	[g]	[-]	[g]	[g]	[-]	[g]	[g]	[g]	[g]	[-]	[-]	[-]
B	5.1	4.9	1.0E-03	4.9	4.4	1.0E-03	0.2	0.5	0.0	0.7	2.9E-01	7.1E-01	7.1E-04
B	4.9	5.0	5.0E-03	4.0	4.6	5.0E-03	0.9	0.4	0.0	1.3	6.8E-01	3.2E-01	1.6E-03
A	5.0	5.0	5.0E-03	3.7	4.2	5.0E-03	1.3	0.8	0.0	2.1	6.2E-01	3.8E-01	1.9E-03
B	4.9	4.9	1.0E-02	3.9	3.0	1.0E-02	1.0	1.9	0.0	2.9	3.4E-01	6.5E-01	6.6E-03
A	4.9	5.0	1.0E-02	3.7	3.0	1.0E-02	1.2	2.0	0.0	3.2	3.8E-01	6.1E-01	6.2E-03
B	5.1	5.1	2.0E-02	3.4	3.2	2.0E-02	1.7	1.9	0.0	3.6	4.7E-01	5.2E-01	1.1E-02
A	5.0	5.0	2.0E-02	4.1	2.7	2.0E-02	0.9	2.3	0.0	3.2	2.8E-01	7.0E-01	1.4E-02
B	4.9	5.0	4.0E-02	1.2	**NP**	**NP**	3.7	4.8	0.2	8.7	4.2E-01	5.5E-01	2.3E-02
A	4.9	4.9	4.0E-02	1.6	**NP**	**NP**	3.3	4.7	0.2	8.2	4.0E-01	5.7E-01	2.4E-02
B	5.0	5.0	1.2E-01	4.2	4.0	1.1E-01	0.8	0.8	0.2	1.8	4.5E-01	4.7E-01	8.6E-02
A	5.1	4.9	1.2E-01	2.2	3.0	1.2E-01	2.9	1.7	0.2	4.8	6.0E-01	3.5E-01	4.8E-02

…Continued

Coord	before sonication			after sonication									
name	m_1^b	m_2^b	γ_2^b	m_1^a	m_2^a	γ_2^a	m_O	m_W	m_S	m	γ_O	γ_w	γ_s
[-]	[g]	[g]	[-]	[g]	[g]	[-]	[g]	[g]	[g]	[g]	[-]	[-]	[-]
A	5.1	5.0	1.6E-01	3.1	3.7	1.5E-01	2.0	1.1	0.2	3.3	6.1E-01	3.2E-01	7.4E-02
B	5.1	5.0	2.0E-01	3.4	2.9	2.1E-01	1.7	1.7	0.4	3.8	4.5E-01	4.5E-01	1.0E-01
A	4.9	5.1	2.0E-01	3.0	3.3	2.0E-01	1.9	1.4	0.4	3.7	5.1E-01	3.9E-01	9.7E-02
B	4.9	5.0	2.4E-01	3.4	2.8	2.3E-01	1.5	1.6	0.6	3.7	4.1E-01	4.4E-01	1.5E-01
A	5.1	5.0	2.4E-01	3.4	3.2	2.3E-01	1.7	1.3	0.5	3.5	4.9E-01	3.8E-01	1.3E-01
B	5.0	5.0	2.8E-01	3.9	3.2	2.8E-01	1.1	1.3	0.5	2.9	3.8E-01	4.5E-01	1.7E-01
A	4.9	5.0	2.8E-01	4.4	4.2	2.8E-01	0.5	0.6	0.2	1.3	3.8E-01	4.4E-01	1.7E-01
B	5.1	4.9	3.2E-01	4.8	4.1	2.9E-01	0.3	0.4	0.4	1.1	2.7E-01	3.8E-01	3.4E-01
A	5.0	5.0	3.2E-01	4.6	4.6	2.9E-01	0.4	0.1	0.3	0.8	5.0E-01	1.7E-01	3.3E-01
B	5.0	5.0	3.6E-01	4.5	4.6	3.5E-01	0.5	0.2	0.2	0.9	5.6E-01	2.3E-01	2.1E-01
A	5.1	5.0	3.6E-01	4.1	4.0	3.5E-01	1.0	0.6	0.4	2.0	5.0E-01	3.0E-01	2.0E-01
A	4.9	5.0	4.0E-01	4.4	4.4	4.0E-01	0.5	0.4	0.2	1.1	4.5E-01	3.3E-01	2.2E-01
B	5.1	5.0	4.4E-01	4.7	4.6	4.5E-01	0.4	0.3	0.1	0.8	5.0E-01	3.4E-01	1.6E-01
A	5.0	5.0	4.4E-01	4.8	4.5	4.5E-01	0.2	0.3	0.2	0.7	2.9E-01	4.6E-01	2.5E-01
A	5.1	5.0	4.6E-01	4.6	4.1	4.7E-01	0.5	0.5	0.4	1.4	3.6E-01	3.7E-01	2.8E-01

The mass fraction of surfactant in the lower layer after sonication was measured using the refractive index. The correlation between the refractive index and the surfactant concentration was drawn in Figure 18. The curve was drawn independently, prior to sonication.

It was possible to make a linear fit the RI to the surfactant concentration. Giving a corresponding linear equation:

$$RI = a\gamma + b \quad \text{<2.6>}$$

After sonication the refractive index values of the surfactant and water mixture were compared with calibration curve and the new surfactant concentration was determined. The new surfactant concentration after sonication (*a*) was found with the refractive index with the following equation:

$$\gamma^a = \frac{RI^a - b}{a} \quad \text{<2.7>}$$

With the data measured in Table 6 it was possible to determine coefficients *a* **(0.00151)** and *b* **(1.3316).** With the coefficients the surfactant concentrations were calculated (Table 7).

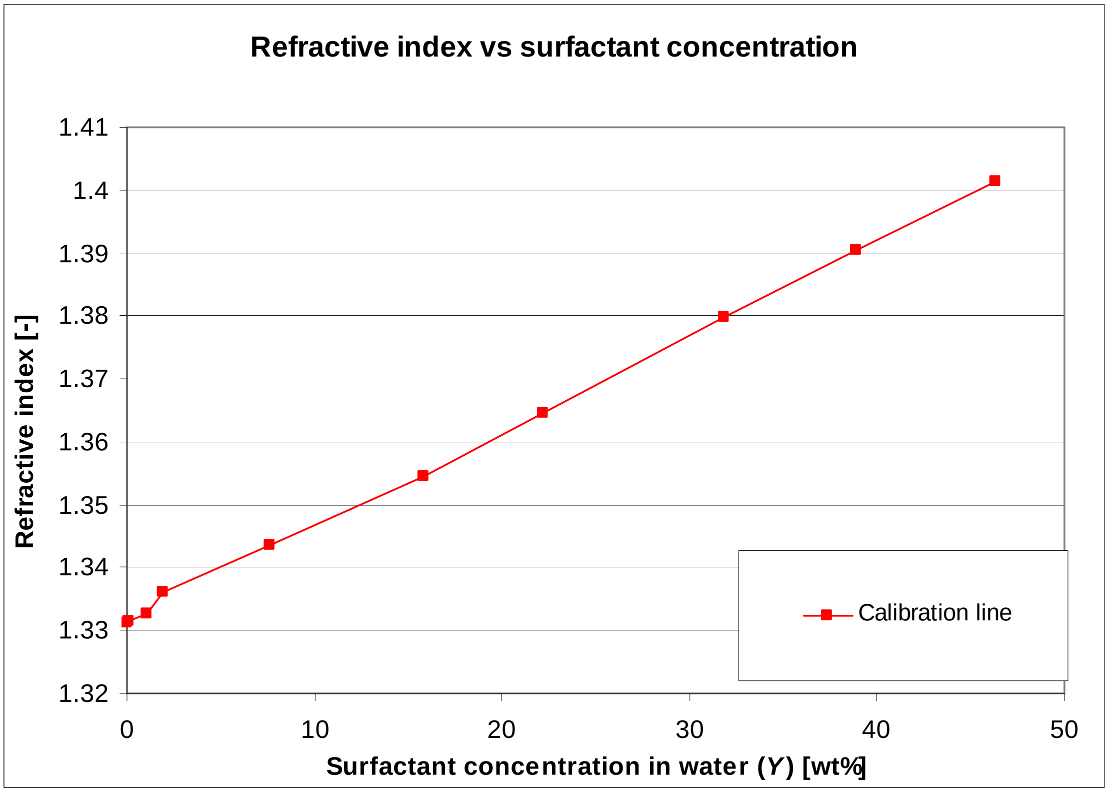

Figure 18: The calibration curve was measured independently, prior to sonication. The blue solid circles are examples of Refractive index measurements of the surfactant solution after sonication.

Table 6: Refractive index (RI) measurements for calibration curve of varying surfactant dilutions. The solutions were untreated (no sonication).

Calibration curve	
y_S	RI
[wt%]	[-]
0.00	1.331
0.05	1.332
0.10	1.332
1.00	1.333
2.00	1.336
8.00	1.344
16.00	1.355
24.00	1.365
32.00	1.380
40.00	1.391
46.31	1.401

Table 7: Calculated surfactant concentrations with the refractive index (RI).

After sonication		
Coordinate	Measured RI	$Y_{S2}{}^{a}$
[-]	[-]	[wt%]
B	1.348	11.1
A	1.355	15.4
B	1.362	20.5
A	1.362	20.3
B	1.366	23.0
A	1.366	22.7
B	1.373	27.8
A	1.373	27.5
B	1.376	29.4
A	1.376	29.4
B	1.385	35.1
A	1.385	35.1
B	1.391	39.1
A	1.391	39.5
B	1.399	44.6
A	1.399	44.6
B	1.403	47.0
A	1.402	46.9

With the mass fraction of the surfactant after sonication it was then possible to calculate the mass and mass-fractions of the three components for the middle phase (Table 5). For a better illustrative representation of the data, the mass fractions of the three components for both coordinate **A** and **B** have been plotted in a ternary diagram (Figure 19). The purple diamonds represent the water and oil phase prior to sonication. The green figures are the mass fractions of coordinate **A** and the red for coordinate **B**. The triangles represent an opaque white emulsion middle phase and the six-stars represent the *gel* middle phase.

It could be observed that even though the coordinates **A** and **B** had identical initial conditions the calculated mass fractions deviated significantly (Figure 19). Two possible arguments for this are: The energy that is focused at the two coordinates is significantly different (contrary to what initially was believed) (chapter 1). Another explanation is that the experimental methods that were applied were not accurate enough to employ a mass balance. In the forthcoming paragraph an uncertainty analysis will give further insight in this.

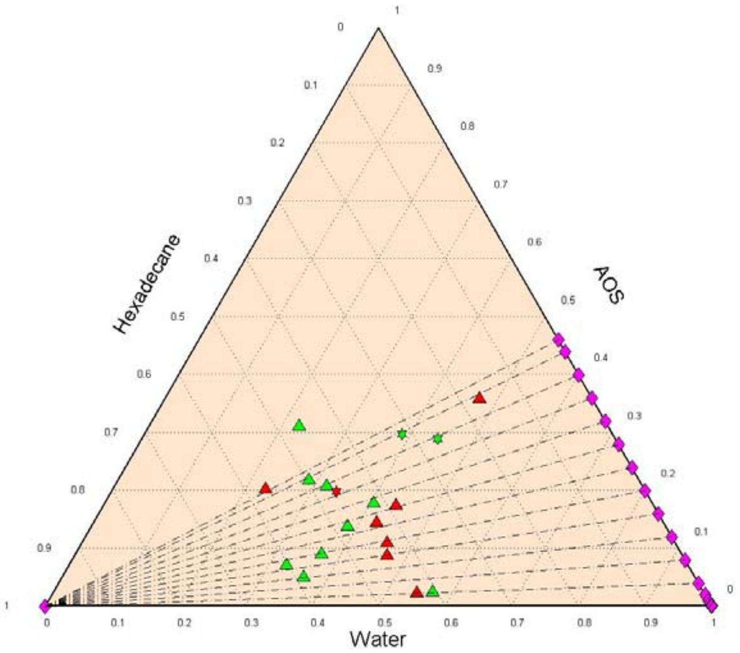

Figure 19: The mass fractions of the three components plotted in a ternary phase diagram. Green markers are from A coordinate and red from B coordinate (see Figure 12 for exact location). The six point stars indicate a gel like middle phase, the triangles that the middle phase is an emulsion.

Experimental error & uncertainty of the mass balance equation

During removal of the existing layer 1 and 2 after the insonication, some of the liquid was left behind (Figure 20). Therefore the error in Δm_1 and Δm_2 is and. We thus have that:

$$\Delta m_1 = m_1^b - m_1^a + \varepsilon_{1,} \qquad \text{<2.8>}$$

Because m_1^a is estimated less than it actually is, and ε_1 is the residue left behind, which leads to an overestimation of Δm_1. Similar for m_2:

$$\Delta m_2 = m_2^b - m_2^a + \varepsilon_2, \qquad \text{<2.9>}$$

When ε_2 is the residual mass left behind is substitution of 2.4 in 2.1, 2.1 and 2.3 it follows that:

$$\begin{aligned} m_O &= \Delta m_1 - \varepsilon_1 = m_1^b - m_1^a - \varepsilon_1, \\ m_W &= m_2^b(1-\gamma^b) - (m_2^a + \varepsilon_2)(1-\gamma^a), \\ m_S &= m_2^b \cdot \gamma^b - (m_2^a + \varepsilon_2)\gamma^a. \end{aligned} \qquad \text{<2.10>}$$

From which follows:

$$m = m_O + m_W + m_S = \\ m_1^b - m_1^a - \varepsilon_1 + m_2^b - m_2^a - \varepsilon_2, \tag{2.11}$$

Which means that:

$$m = \Delta m_1 + \Delta m_2 - \varepsilon = \Delta m - \varepsilon \\ \text{When } \varepsilon = \varepsilon_1 + \varepsilon_2, \text{ and } \Delta m = \Delta m_1 + \Delta m_{2.} \tag{2.12}$$

When substituting equations 2.10 and 2.11 in equation 2.5 the errors of the mass fractions are found:

$$\gamma_O = \frac{m_O}{m} = \frac{m_1^b - (m_1^a + \varepsilon_1)}{m + \varepsilon}, \\ \gamma_W = \frac{m_W}{m} = \frac{(1-\gamma^b)m_2^b - (1-\gamma^a)(m_2^a + \varepsilon_2)}{m + \varepsilon}, \\ \gamma_S = \frac{m_S}{m} = \frac{\gamma^b m_2^b - \gamma^a (m_2^a + \varepsilon_2)}{m + \varepsilon}. \tag{2.13}$$

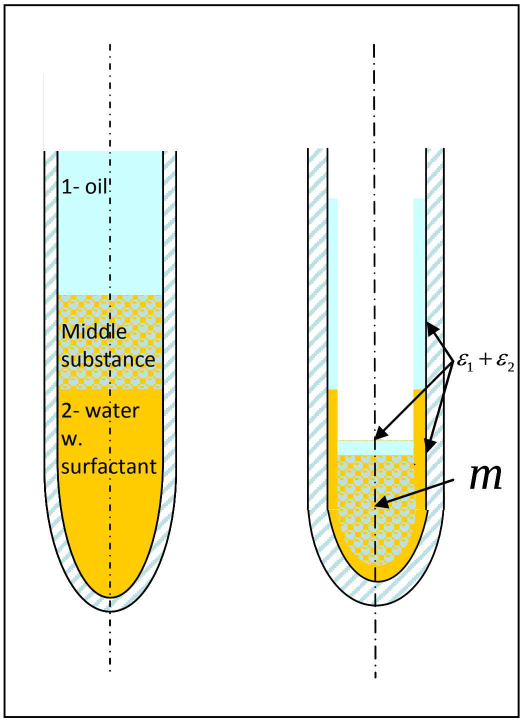

Figure 20: A schematic representation of the experimental error when estimating the mass of the middle phase. It can be observed that as the mass of the middle substance becomes smaller the relative error becomes bigger. Furthermore it can be seen that the mass of the middle substance is over estimated due to ε_1 and ε_2.

The uncertainty (absolute) to the mass fraction calculation is found by subtracting the mass fraction with experimental error (γ^{ε}) from solution without the error (γ):

$$error = \left|\gamma - \gamma^{\varepsilon}\right|, \qquad < 2.14>$$

Subsuming equation 2.18 in 2.14 and having done the same for water and surfactant gives the following equations:

$$\begin{aligned} error_O &= \left|\gamma - \gamma^{\varepsilon}\right| = \frac{m_1^b - (m_1^a + \varepsilon_1)}{m + \varepsilon} - \gamma_O^{\varepsilon}, \\ error_W &= \frac{(1-\gamma^b)m_2^b - (1-\gamma^a)(m_2^a + \varepsilon_2)}{m + \varepsilon} - \gamma_W^{\varepsilon}, \\ error_S &= \frac{\gamma^b m_2^b - \gamma^a (m_2^a + \varepsilon_2)}{m + \varepsilon} - \gamma_S^{\varepsilon}, \end{aligned} \qquad <2.19>$$

When for example the results of the 46wt% surfactant concentration are used (m_1^b=5.1g, m_1^a=4.6g, m=1.4g and γ_O^{ε}=0.36, last row, Table 5) to calculate the error the following is obtained:

$$error_O = \frac{5.1 - (4.6 + \varepsilon_1)}{1.4 + \varepsilon} - 0.36,$$

Assuming a worst case scenario of ε_1=ε_2=0.1g (and ε= ε_1+ε_2) then the $error_O$ becomes:

$$error_O = \frac{5.1 - (4.6 + 0.1)}{1.4 + 0.2} - 0.36 = 0.10.$$

Uncertainty calculations have been done for all components and for all experiments. The results are shown in Table 8. It is important to note that the uncertainty has an inverse relationship with the mass of the middle substance. This behaviour has been illustrated in Figure 21.

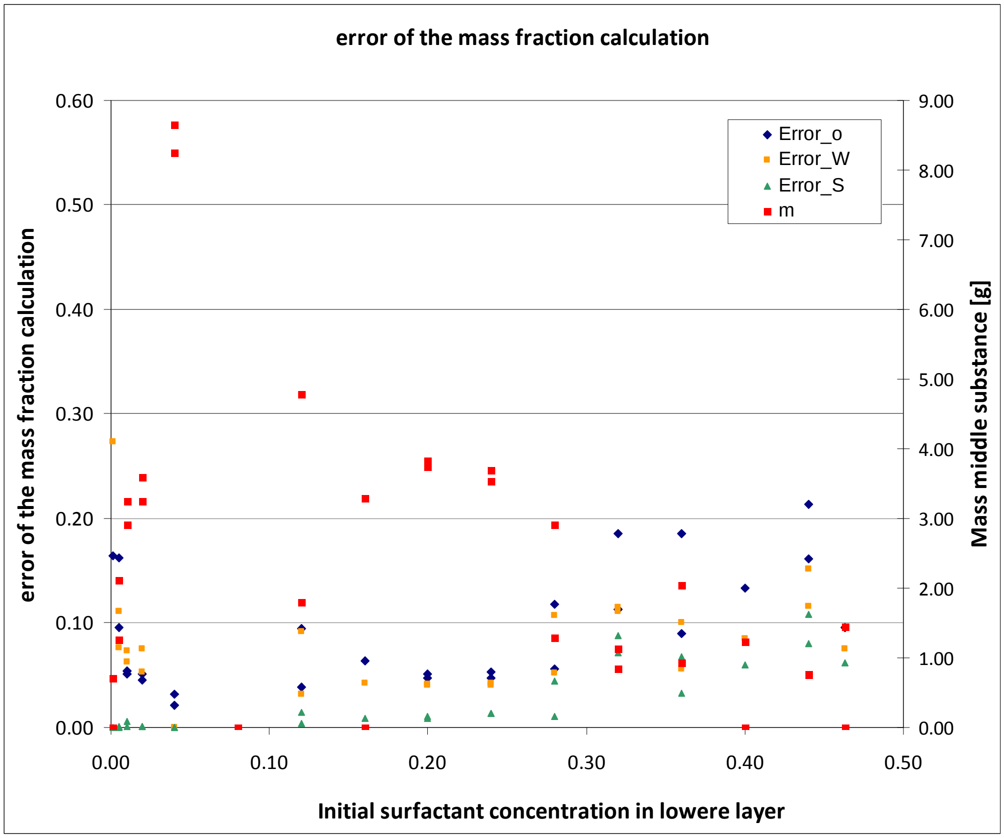

Figure 21: Uncertainties of the relative mass fractions of the components water (W orange square), oil (O, blue diamond), and Surfactant (S, green triangle). The mass of the middle substance has been plotted (red squares) to illustrate the behaviour of the uncertainty with respect to the mass of the middle substance. as a worst case scenario the residual error ($\varepsilon_1 = \varepsilon_2$), of the oil, the value of 0.2g was assumed.

Table 8: The errors (ξ) of the mass fractions (γ) of the individual components oil (O), water (W), and Surfactant (S) . The exact mass fraction (γ), has been determined with the calculated mass fraction (γ^{ε}) and the assumed mass errors (ε_1 and ε_2) of 0.10 g.

uncertainty								
γ_O^{ε}	γ_O	*error* $_O$	γ_W^{ε}	γ_W	*error* $_W$	γ_S^{ε}	γ_S	*error* $_S$
[-]	*[-]*	*[-]*	*[-]*	*[-]*	*[-]*	*[-]*	*[-]*	*[-]*
0.25	0.09	0.16	0.75	0.47	0.27	0.00	0.00	0.00
NA	**NA**	**NA**	**NA**	**NA**	**NA**	**NA**	**NA**	**NA**
0.68	0.52	0.16	0.32	0.20	0.11	0.00	0.00	0.00
0.61	0.52	0.10	0.39	0.31	0.08	0.00	0.00	0.00
0.34	0.29	0.05	0.65	0.58	0.07	0.00	0.01	0.01
0.38	0.33	0.05	0.61	0.55	0.06	0.01	0.01	0.00
0.47	0.42	0.05	0.52	0.46	0.05	0.01	0.01	NA
0.28	0.24	0.05	0.71	0.64	0.07	0.01	0.01	0.00
0.42	0.40	0.02	0.56	0.56	0.00	0.02	0.02	0.00
0.41	0.38	0.03	0.57	0.57	0.00	0.02	0.02	0.00
NA	**NA**	**NA**	**NA**	**NA**	**NA**	**NA**	**NA**	**NA**
NA	**NA**	**NA**	**NA**	**NA**	**NA**	**NA**	**NA**	**NA**
0.44	0.35	0.09	0.47	0.38	0.09	0.09	0.07	0.01
0.60	0.56	0.04	0.35	0.32	0.03	**0.05**	0.04	0.00
NA	**NA**	**NA**	**NA**	**NA**	**NA**	**NA**	**NA**	**NA**
0.62	0.55	0.06	0.31	0.27	0.04	**0.07**	0.06	0.01
0.45	0.40	0.05	0.45	0.40	0.04	**0.10**	0.10	0.01
0.51	0.46	0.05	0.39	0.35	0.04	0.10	0.09	0.01
0.41	0.37	0.05	0.44	0.39	0.04	0.15	0.13	0.01
0.50	0.44	0.05	0.37	0.33	0.04	**0.13**	0.12	0.01
0.38	0.32	0.06	0.45	0.39	0.05	0.17	0.16	0.01
0.38	0.26	0.12	0.43	0.33	0.11	0.19	0.15	0.04
0.26	0.14	0.11	0.41	0.30	0.11	0.33	0.26	0.07
0.46	0.28	0.19	0.23	0.11	0.11	0.31	0.22	0.09
0.55	0.37	0.19	0.24	0.14	0.10	0.21	0.14	0.07
0.50	0.41	0.09	0.30	0.24	0.06	0.20	0.16	0.03
NA	**NA**	**NA**	**NA**	**NA**	**NA**	**NA**	**NA**	**NA**
0.46	0.32	0.13	0.31	0.23	0.09	0.23	0.17	0.06
0.54	0.33	0.21	0.29	0.17	0.12	0.17	0.09	0.08
0.27	0.11	0.16	0.44	0.29	0.15	0.29	0.18	0.11
NA	**NA**	**NA**	**NA**	**NA**	**NA**	**NA**	**NA**	**NA**
0.36	0.26	0.10	0.36	0.28	0.08	0.28	0.21	0.06

Thermogravimetric analysis of the gel Mass fractions

Thermogravimetric analysis (TGA) is a method where a sample is heated at constant rate (^{O}C/min) on a very accurate scale. To prevent oxidation this is often done in a Nitrous environment. By analyzing the weight change and the derivative of the weight change with respect to the temperature. The weight of the sample can decrease for instance due to evaporation or decomposition but it can also increase due to oxidation. The temperatures at which certain reactions take place are often specific for the components in the sample.

A TGA (PerikinElmer TGA7 thermogravimetic analyzer, + 0.1 wt%) was performed on one of the gel samples that was produced after sonicating 5g of hexadecane and 46 wt% surfactant solution for 30 min (identical as described in previous paragraphs). In order to predict the behaviour of water, alpha-olefin-sulphonate (surfactant) and hexadecane at certain temperatures the components were analyzed separately prior to sonication. The hexadecane (green curve Figure 22) was of identical quality as was used when fabricating the gel. It could be seen that the hexadecane started to evaporate at around 110^{O}C and had completely evaporated at around 200^{O}C. The 46 wt% surfactant solution (blue curve Figure 22) that was analyzed was identical to the surfactant solution that was used when fabricating the gel. The demineralised water within the solution started to evaporate immediately (room temperature) and it is expected that the water was completely evaporated at (180^{O}C). At this temperature the residual weight% was around 46 wt% as expected. The residual surfactant components (consists of a mixture of components) than start to evaporate/decompose at around 270^{O}C. AT around 400^{O}C this behaviour diminishes and at 900^{O}C the residual 10 wt% of components (probably heavy carbon fraction) remains behind.

The gel that was analyzed had a 46 initial wt% surfactant concentration and showed a remarkably similar pattern to the untreated surfactant solution. This suggests that the gel and the surfactant solution were very similar in make. Between 180^{O}C and 270^{O}C is the only temperature range where they significantly differ with about 5 wt%, this is probably the hexadecane fraction of the gel.

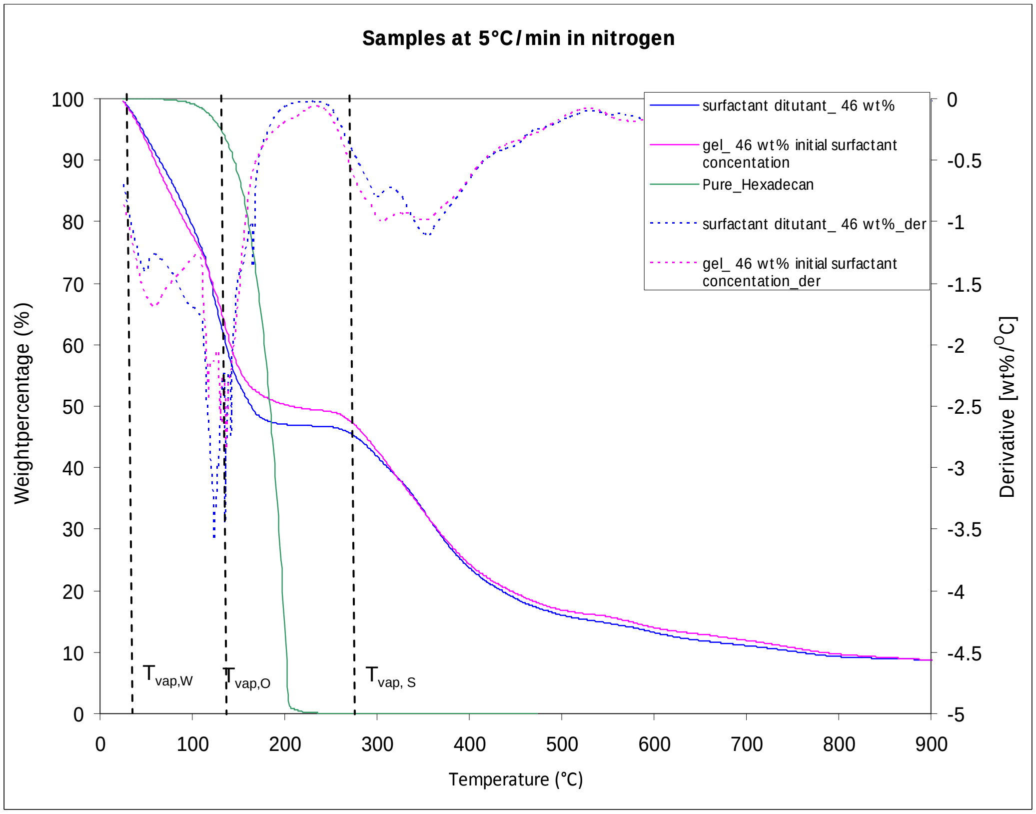

Figure 22: Thermogravimetric analysis. The pink solid lines are the TGA curves and the dotted (coloured) are for the derivatives. The pink line is a gel sample. The blue is a 46wt% surfactant dilutant. As it has it has the gel used a similar surfactant dilution it can be used for calibrating the gel TGA. The hexadecane curve (green line) has a similar purpose. The black, striped, vertical lines indicate at which temperature the indicated component starts to evaporate (T_{vap}).

Optical analysis of a freeze-dried gel sample with the Scanning Electron Microscope

Freeze drying

The aim is to visually analyze the cross linking properties of the gel. As the SEM is incapable of showing any contrast between the solvent and the cross linked structure it is imperative that the solvent is removed prior to the analysis. It is possible to remove the solvent by heating the gel-like sample and thereby removing it by evaporation. The method generally damages the cross linked structure however due to the capillary forces that are exerted upon the pores[24]. An alternative is, freeze drying. After freezing the sample the solvent is removed by sublimation. To remove the solvent (water) from the gel a Mini Lyotrap^{TM} Freeze Dryer was used with an Edwards^{TM} RV8 Vacuum pomp attached to it. The sample that was dried was a gel that was fabricated by sonicating 5g of hexadecane and 5g of 46% wt surfactant solution (demineralised water as solvent) for 30 min. The gel sample was freeze dried over a period of 4 weeks and was assumed completely dry.

Analyzing a freeze dried gel sample with a Scanning Electron Microscope

The freeze dried sample was analyzed with a scanning electron microscope. By scanning the surface with a high energy beam of electrons in a raster pattern the SEM produces an image. The electrons interact with the atoms that make up the sample thereby producing a signal that contains information about the sample (gel's) topography, composition and other properties.

Images were made of 34 to 2000x magnifications (Figure 23). It could be noted that as was suspected a clear internal structure was visible at all magnifications.

It was furthermore interesting to note that from the SEM images a tremendous porosity could be observed. At low magnification (< 100x) large spherical pores could be witnessed with smooth surfaces. The spherical pores had a diameter varying from 50 to 500 µm. At low magnifications (<100x) the surface of the pores appeared to be smooth an amorphous. At damaged parts of the matrix and at higher magnifications (>100x) the matrix appeared to be made up of a smaller porosity. The secondary porosity was wormhole shaped and had a radial alignment towards the centre of the larger porosity. The smaller pore structures had a diameter varying from 1 to 3 µm (Figure 23 *f*).

It is conceivable that is possible to correlate the fine structure of the matrix to the low mass fraction of hexadecane that was observed from the TGA (Figure 22). When it is assumed that all the free water has evaporated during the freeze drying, it follows that the matrix consists of dominantly surfactant and hexadecane.

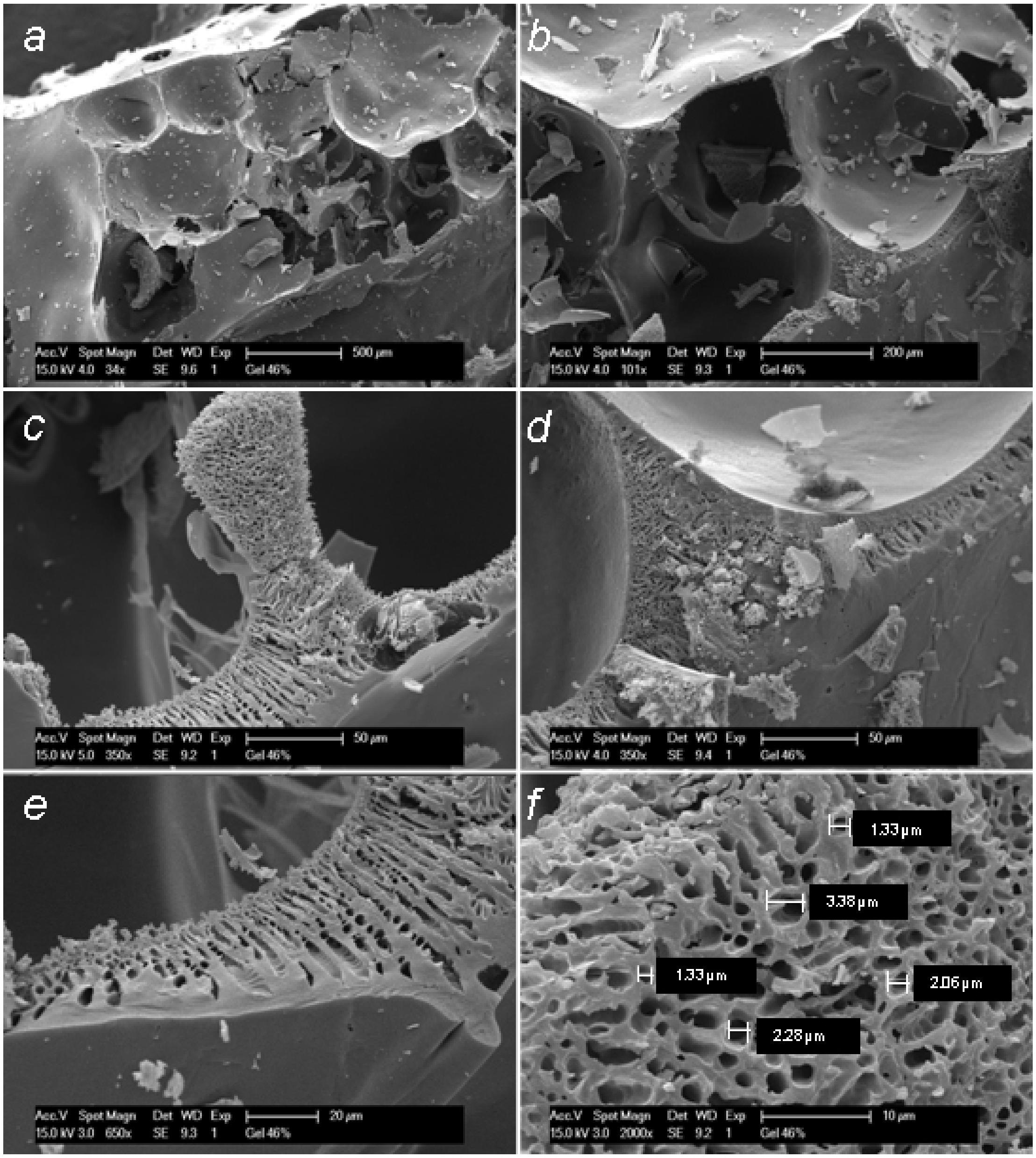

Figure 23: Images made of a freeze dried gel. The gel was fabricated with 46 wt% surfactant (AOS) water mixture. In a and b large pores kan be observed (r=± 200 µm). When taking a closer look at the matrix that build the pores (c-f) these apear to contain a sencondary pore network. This secondary pore network apears to have a wormhole-like strucure (e) with a radial alignment towards the centre of the larger pores. The secondary pores have a diameter ranging from 1–3 µm. It is assumed that the liquid that was originally in the pores was water.

3.5 Discussion

Ultrasound was an efficient emulsifier. Test tubes with 5 g of oil phase and 5 g of water phase were sonicated for 30 min. A middle phase was present in every test tube that had been sonicated. Depending on the concentration of surfactant used results in different quantities and different types of middle phases. The phases that were formed were stable for the duration of the study (< 4 months). Two distinctly different phases could be recognized: an opaque white o/w emulsion could be observed after sonication when the surfactant concentration of the water phase was below 44 wt%. The mass of the middle phase varied but there appeared to be an optimum surfactant concentration when emulsification efficiency is highest.

The other phase that had been observed was a translucent, amber coloured, semi-solid material. The gel like middle phase formed at higher surfactant concentrations (>44 wt%) and had comparable Thermogravimetric characteristics to the untreated surfactant solution. This suggests that probably very little hexadecane (< 5wt%) was present in the gel sample.

From the images taken from SEM two different types of pores were observed at two different magnifications. The first one was spherical in shape and 50 to 500 µm in diameter. The second could be found in the walls of the first pores. These were smaller in size (1-3 µm in diameter and approximately 50 µm in length) and were wormhole in shape. They had a radial alignment towards the centre of the larger pores.

4. Conclusions

- Ultrasound Increases the dissolution rate of sodium chloride
- The ultrasound enhanced dissolution rate of salt can be used to characterize the ultrasonic bath
- Cavitation is present in the ultrasonic bath and it is likely that it enhances the dissolution of salt
- The emulsions form easily under the acoustic stimulation, hence application to mobility control or other EOR related applications could be feasible.
- Mass balance that is used through for the calculation of the mass fractions of the middle substance is a quick and efficient method. The error of the calculation increases however when the mass of the middle substance becomes smaller.
- From the results gathered from TGA it is observed that the mass fraction of the hexadecane in the gel is relatively small.
- The gel-like substance has a distinct three dimensional structure. This suggests that the substance is a gel.

5. Recommendations

- Because of the high precision and repeatability that an experimental set up demands the ultrasonic bath is not recommended as an acoustic source.
- It is recommended to design an experiment employing a different, proven method to characterize the energy distribution in the ultrasonic bath to the determine the quality of acoustic dissolution of salt method
- The next recommended step in for this study would be to:
    - A study of the effect of ultrasound in an porous media and the effect it has on two immiscible fluids
    - The effect of a porous media on the formation of the gel-like substance.
    - An in depth study of the rheology of the emulsions that form under influence of ultrasound (droplet size distribution, viscosity, etc).

References

---

[1] Nikolaevskiy V.N., Inst. Of Phsics of the earth, Russian Academy of Sciences; Lopukhov G.P, Krylov All-Russian Scientific oil-gas Inst; Yizhu-Liao M.J. Economides, Texas A&M U: *Residual Oil reservoir recovery with seismic vibrations.* SPE Production & Facility (Journal, VOl. 11, Nr. 2) © 1996 Society of Petroleum Engineers.

[2] Iassonov P.P., Beresnev I.A., Department of Geological and Atmospherical Sciences, Iowa State University, USA: *A model for enhanced fluid percolation in porous media by application of low-frequency elastic waves.* © American Geophysical Union.

[3] Roberts P.M., Los Alamos National Laboratory, New Mexico, US., Esipov I.B., N.A Acoustic Institute, Moscow, Russia, Majer E.L., Lawrence Berkley National Lab., Cal, US.: *Elastic wave stimulation of oil reservoirs.*(c) Society of Exploration Geophysicists.

[4] Besnev I.A., Physics of the Earth, Russian Acadamy of science, Mosscow, Johnson P.A., GeoEngineering group, Los Alamos National Laboratory: *Elastic-wave stimulation of oil production: A review of methods and results.* Geophysics, Vol 59, No 6 June 1994.

[5] Towler B.F., Chejara A.K., Mokhatab S., University of Whyoming, USA: *Experimental investigation of ultrasonic waves effects on wax deposition during crude-oil production.* © 2007 Society of petroleum engineers.

[6] Cobos S., Carvalho M.S., Alvarado V.: *Flow of oil-water emulsions through a constricted capillary.* © 2009 Elsevier, Oxford.

[7] Fink J.K.: *Oil field chemicals.* © 2003 Elsevier Science USA. Gulf Professional Publishing

[8] Suslick K.S., Didenko Y., Fang M.M., Hyeon T., Kolbeck K.J., McNamara III W.B., Mdleleni M.M., Wong M.: *Acoustic cavitation and its chemical consequences.* School of chemical sciences, University of Illinois. Phil. Trans. Roy. Soc. A (1999), in Press, Great Brittan

[9] Azar L. (President and owner of PPB Megasonics): *Cavitation in Ultrasonic cleaning and cell disruption.* Controlled environments www.cemag.us, Feb 2009

[10] Suslick K.S., Price G,J.: *Applications of ultrasound to material chemistry.* Annu. Rev, Mater. Sci. 1999. 29:295-326.

[11] Brennen C.E.: *Cavitation and Bubble Dynamics*. Oxford University press 1995

[12] Chivate M.M., Pandit A.B., Department of Chemical Technology, University of Bombay, Bombay: *Quantification of cavitation intensity in fluid bulk.* Ultrasonics sonochemistry 1995 vol 2 no. 1. Elsevier Sci. 1995

[13] Koyler J.M., Passchier A.A.: *New wrinkles in evaluating ultrasonic tanks.* Clean tech central

[14] Lide D.R.,: H*andbook of chemistry and physics.* 27th edition. Chemical Rubber Company

[15] Schramm L.L., Tadros Th. F.: *Surfactants: Fundamentals and applications in the oil industry.* Cambridge University Press © 2000

---

[16] Meyers D.,: *Surfactant science and technology.* Wiley inner science. A john wiley & sons. Inc., Publication © 2006 3rd edition.

[17] Tadros Th.F.: *Applied Surfactants: Principles and applications.* Wiley-VCH Verlag GmbH & Co. KGaA. © 2005

[18] Schultz S., Wagner G., Urban K., Ulrich J.: *High-Pressure Homogenization as a Process for Emulsion formation.* Chem. Eng. Techn.. Wiley-VCH Verlag GmbH & Co. KGaA © 2004, 27, No. 4

[19] Bechtel S, Gilbert N. Gunter Wagner H.: *Grundlagenuntersuchungen zur Herstellung von Oll /Wasser-Emulsionen im Ultraschallfeld.* Chemie Ingenieur Technik (71). Wiley-VCH Verlag GmbH & Co. KGaA © 1999

[20] Abismail B., Canselier J.P., Wilhelm A.M., Delmas H., Gourdon C.L *Emulsification by ultrasound:drop size distribution and stability.* Ultrasonic Sonochemistry 6 (1999) 75-83. © Elsevier science BV.

[21] Abismail B., Canselier J.P., Wilhelm A.M., Delmas H., Gourdon C.L: *Emulsification process: on-line study by multiple light scattering measurements.* Ultrasonic Sonochemistry 7 (2000). © 2000 Elsevier science BV

[22] Cucheval A., Chow R.C.Y.: *A study on the emulsification of oil by power ultrasound.* Ultrasonic Sonochemistry 15 (2008). © Published by Elsevier B.V.

[23] Viyoch J.. dept of pharmaceutical Techn, Emulsions, http://www.surfatech.com/pdfs/emulsions.pdf

[24] Job N. Thery A., Pirard R., Marien J., Kocon L., Rouzaud J-N., Beguin F., Pirard J-P.: *Carbon Aerogels, cryogels and xerogels: Influence of the drying method on the textural properties of the porous materials.* © 2005 published by Elsevier B.V